MEASUREMENTS ON THE FLOW AND ACOUSTIC PROPERTIES OF A MODERATE REYNOLDS NUMBER SUPERSONIC JET

By

TIMOTHY RAY TROUTT

Bachelor of Science
Oklahoma State University
Stillwater, Oklahoma
1972

Master of Science
Oklahoma State University
Stillwater, Oklahoma
1974

Submitted to the Faculty of the
Graduate College of the
Oklahoma State University
in partial fulfillment of
the requirements for
the Degree of
DOCTOR OF PHILOSOPHY
July, 1978

MEASUREMENTS ON THE FLOW AND ACOUSTIC PROPERTIES OF A MODERATE REYNOLDS NUMBER SUPERSONIC JET

Thesis Approved:

Dennis K McLaughlin
Thesis Adviser

W. A. Tiederman

Ladislaus J. Fila

D D Fisher

Norman N Durham
Dean of the Graduate College

ACKNOWLEDGMENTS

The author wishes to express his appreciation to his major adviser, Dr. Dennis K. McLaughlin, and to his other committee members, Dr. Ladislaus J. Fila, Dr. Donald C. Fisher, and Dr. W. G. Tiederman, for their advice and guidance regarding this study.

Appreciation is also extended to Mr. J. L. Stromberg, Mr. J. D. Swearingen, and Dr. G. L. Morrison for their assistance with the experiments and for their contributions toward the design and construction of the experimental facility. Thanks is also extended to Mr. D. G. Bogard for his helpful comments on the research.

The author would also like to express his gratitude toward Miss Elizabeth Bastion for her help with the rough draft typing, and to Velda Davis and Debbie Reimer for the final typing.

Finally, the author would like to recognize the financial support of the National Science Foundation (Grant No. ENG 75-21405) and the National Aeronautics and Space Administration (Grant No. NSG 1467).

TABLE OF CONTENTS

TABLE

LIST OF FIGURES

NOMENCLATURE

a_o	speed of sound in the ambient air
A_m	mass velocity fluctuation sensitivity coefficient
A_T	stagnation temperature fluctuation sensitivity coefficient
c	axial wave speed
D	nozzle exit diamter
e	hot-wire voltage
$E_{K.D.}$	kinetic energy flux
f	frequency (Hz)
k	complex wave number
k_i	imaginary part of the complex wave number
k_r	real part of the complex wave number
M	Mach number
n	azimuthal mode number
P	pressure
P_{atm}	standard atmospheric pressure
P_c	test chamber pressure
P_n	static nozzle exit pressure
r	radial distance from jet centerline, cylindrical coordinate system
R	radial distance from center of jet at nozzle exit, spherical coordinate system
Re	Reynolds number $\frac{U_o D}{\nu}$

Rg	gas constant
St	Strouhal number, fD/U_o
T	temperature
u	axial velocity
U_o	jet centerline exit velocity
v	radial velocity
x	downstream distance from the nozzle
y	vertical distance from the centerline
z	horizontal distance from the centerline
α	angle at which acoustic wavefronts are inclined to x axis
β	angular coordinate in spherical coordinate system, measured from x axis
γ	ratio of specific heats
θ	azimuthal angle
ν	kinematic viscosity
λ	axial wavelength
μ	Mach angle
ρ	density
τ	period of the organized wave
φ	relative sensor phase angle
ω	frequency (radians/sec)
$( )_t$	quantity evaluated at stagnation conditions
$( )_o$	quantity evaluated at jet exit
$(\bar{})$	time average of quantity
$( )_{rms}$	root mean square of quantity
$\langle \rangle$	phase average of quantity

$( )'$ total fluctuation, $( )' = (\sim) + ( )''$

$( )''$ random portion of fluctuation

$(\sim)$ periodic portion of fluctuation

CHAPTER I

INTRODUCTION

A. Background

High speed exhaust jets from turbojet aircraft are one of the major contributors to present day noise pollution. Past attempts to control the noise from high speed jets using a trial and error approach to modification of the jet flow have met with limited success. To devise effective remedies for reducing jet noise production, it appears essential that a sufficient understanding of the noise generation processes be developed. To this purpose, a great amount of research activity has been devoted over the past twenty-five years.

The first effort at developing a theoretical basis for aerodynamic noise generation was produced in the early 1950's by M. J. Lighthill (1, 2). By rewriting the governing equations for arbitrary fluid motion, Lighthill obtained the equations for acoustic wave propagation due to external stresses composed of fluctuating flow quantities. Lighthill's basic approach was extended to high speed jets by Ffowcs Williams (3). His analysis predicted that eddies convecting supersonically with respect to the surrounding air would radiate noise in the form of Mach waves. This eddy Mach

wave concept had been proposed earlier by Phillips (4) for the noise produced from a supersonic free shear layer. Improvements and extensions upon Lighthill's subsonic theory were also made by a number of authors (5, 6, 7, 8). These early theories of aerodynamic noise production provided considerable understanding of the noise generation processes. However, since at that time little was known about the character of turbulent flows, efforts at predicting the noise producing quantities were relegated to simple scaling models.

Originally, it was assumed that the flow fluctuations in turbulent free shear flows occur in irregular patterns. Within the past 10 years, however, numerous experimental results have indicated that a large scale coherent fluctuation plays an important role in the development of free shear flows. This coherent structure has been established quite clearly in low speed flows. Shadowgraphic observations of free shear layers by Brown and Roshko (9) displayed a wave-like undulation of the shear layer which first appears at low Reynolds numbers, but persists as the Reynolds number is increased and remains a dominant feature of the flow even at Reynolds numbers where the flow is commonly assumed to be fully turbulent. Using dye to mark the large scale structures in a shear layer produced by two streams of different velocity water, Winant and Browand (10) photographed the interaction of the large scales. They found that the large structures tended to pair as they convected downstream. Based on these results, they proposed this pairing process as the primary

mechanism for turbulent shear layer growth. Crow and Champagne (11) artificially excited a turbulent low speed air jet using an acoustic driver. They observed that the jet preferentially amplified axisymmetric wave-like disturbances near St = 0.30, and that the amplified disturbances had phase velocities which corresponded to linear stability theory predictions. Slightly later, Lau and Fisher (12) established the existence of orderly structure in an unexcited subsonic jet using conditionally sampled hot-wire signals. Recently, Chan (13) enlarged upon Crow and Champagne's experimental measurements using a number of acoustical drivers positioned at the nozzle exit to excite various azimuthal disturbance modes of a low speed axisymmetric jet. Chan also used an energy integral mathematical formulation to predict the growth and development of the wave disturbances. Close agreement was found by Chan between his theoretical predictions and experimental measurements.

Evidence of noise generating coherent fluctuations has also been found in high speed flows by several researchers. Mollo-Christensen (14) was one of the first to find indications of coherent noise generators when he observed that the noise from a high speed jet (M = 0.9) seemed to be produced in discrete wave packets. Recently, Moore (15) determined from an extensive experimental study that large scale instability waves at high subsonic Mach numbers apparently govern the noise production processes. Bishop, Ffowcs Williams, and Smith (16) also found some evidence to indicate that the

noise from supersonic jets was produced by large scale wave-like disturbances within the flow. Shadowgraphic and holographic visual techniques (17, 18) have also indicated that coherent disturbances exist within supersonic jets. Intense acoustic wave fronts appearing as Mach waves were observed to be generated by these disturbances.

Directional microphone measurements made by Laufer (19) have shown that the dominant noise from supersonic jets of Mach numbers above 2 is generated in two localized regions near the end of the potential core. Laufer believes two types of noise generation processes may be occurring in the jet. The noise from the upstream region is attributed to Mach wave generation from the supersonically convecting large scale disturbances. The noise from the downstream region is postulated to be caused by the vortex pairing process uncovered by Winant and Browand. One of Laufer's students, Dutt (20), has used microphone cross-correlation measurements of the noise from a M = 2.0 jet to determine that the coherent disturbances radiate noise predominantly at angles less than 45^{o} to the jet axis. (The most intense region of noise propagation from jets of Mach numbers between 1.5 and 2.5 occurs at angles less than 45^{o} from the jet axis.)

A number of theoreticians, upon observing the fact that the large scale disturbances in the turbulent flows appear similar to instabilities of transitional flows, have used hydrodynamic stability models to predict the development of the coherent noise generators (21-26). Of these theoreticians,

Morris and Tam (26) have developed the most comprehensive noise prediction model. Their work uses a linearized instability wave theory with inputs from turbulent mean flow profiles to predict the growth and decay of the coherent disturbances. The noise produced by the instability wave is then calculated using a matched asymptotic expansion method. Comparisons between their computed results and the experimental measurements of Yu and Dosanjh (27) for the radiated noise field of a M = 1.5 jet at selected frequencies show excellent agreement.

These results indicate that coherent flow fluctuations play an important role in the noise generation mechanisms of supersonic jets. However, at the present time there exists a need to develop a more substantial experimental base upon which checks and refinements of mathematical models may be made. The present experimental study is intended to contribute to the development of this base.

B. Subject of Research

The present measurements represent an extension of the ongoing OSU high speed jet noise research program. Over the last 4 years, extensive experimental measurements of the flow and acoustic properties of low Reynolds number (Re = 2,000 to 10,000) high speed jets (M = 0.9 to 2.5) (28-31) have been conducted in our laboratory. A number of experimental advantages are obtained with the low Reynolds number jets. The low density of the flows reduce the dynamic stresses on

the hot-wire probes so that standard hot-wire anemometry techniques can be employed to measure flow fluctuations. The flows can be artificially excited using a glow discharge device (see General Facility section for more details). Also due to the fact that a few discrete frequencies dominate the flow fluctuations, noise generation processes can be analyzed with less confusion than in turbulent jets.

The major objective of these measurements has been to identify the role of large scale flow instabilities in the noise production process. At low Reynolds numbers, it was found that large scale instabilities (wavelengths on the order of several jet diameters) dominate the flow fluctuations. It was also observed that the non-dimensional frequencies of these instabilities were close to the peak frequency of the dominant noise from turbulent high speed jets. The noise produced by these wave-like instabilities was found to have amplitudes and directivity patterns closely comparable to high Reynolds number jets ($Re \approx 2 \times 10^6$). These results not only demonstrate that coherent flow disturbances are powerful noise generators, but also constitute additional evidence indicating that coherent disturbances play an important role in turbulent high speed jet noise production.

The present research reports on the initial OSU experiments on the flow and acoustic properties of a moderate Reynolds number supersonic jet ($Re \approx 70{,}000$, $M = 2.1$). The overall goal of this research was to develop some understanding of the flow and noise generation processes occurring in what

normally could be termed a turbulent high speed jet. The Reynolds number of this flow was chosen as a compromise between the high Reynolds number flows where experimental difficulties are considerable and the low Reynolds number flows which do not exhibit the complex flow behavior of interest.

At the chosen Reynolds number flow condition of 70,000, it was found that the flow fluctuations in the shear layer saturate in amplitude between 3 and 4 diameters downstream of the exit, and that the frequency spectra of the flow fluctuations and the radiated noise are broad (see Results section for details). These properties can be contrasted to low Reynolds number measurements (Re = 7900) where the properties of the same Mach number jet show flow and noise spectra dominated by discrete frequencies and flow fluctuation amplitudes which saturate between 8 and 10 diameters downstream of the nozzle exit (30).

Two experimental advantages of the low Reynolds number jets were retained by operating at the moderate Reynolds number condition. These advantages were the capability to use standard hot-wire probes to measure the flow fluctuations and the capability to excite the jet artificially.

The jet was artificially excited by generating a controlled disturbance near the nozzle exit using a glow discharge. Wavelengths of the excited disturbances were measured by cross-correlating the sensor signal with the exciter signal. Amplitude measurements of the excited

disturbance were made using the exciter signal as a trigger for phase averaging the sensor signals (see Phase Averaging section for details on phase averaging techniques).

C. Research Objectives

The overall goal of the present experimental study was to increase the understanding of the noise production processes in supersonic jets with particular emphasis on the nature of the coherent noise generators. In order to pursue this goal an experimental study was carried out on the flow and acoustic properties of a Re = 70,000; M = 2.1 jet. The specific objectives of this study are listed as follows:

1. To obtain information on the natural flow processes occurring in the jet.
2. To obtain information on the properties of the acoustic radiation generated by the natural jet.
3. To artificially excite the jet and evaluate the effects of the excitation on the flow and acoustic fields of the jet.
4. To measure the characteristic properties of the excited disturbances such as wavelengths, wavespeeds, and amplitudes.
5. To measure the characteristic properties of the near field acoustic radiation generated by the excited disturbances (such as wavelengths, wave angles, and amplitudes).

The results of the excitation experiments should be regarded as applying directly only to an artificially forced jet. However, it does not seem unreasonable to suspect that many of the properties of the artificial disturbances such as wavelength, wavespeed, and noise production mechanisms may also be characteristic of the postulated naturally occurring coherent disturbances. Following this rationale several previous investigators have used artificial excitation techniques to investigate the coherent structure in turbulent flows. Most notable with respect to the present work were Crow and Champagne (11), Moore (15), and Chan (13), all in the case of subsonic jets.

CHAPTER II

EXPERIMENTAL APPARATUS

A. General Facility

This study was carried out in the Oklahoma State University high speed jet noise test facility. A schematic of the overall facility is shown in Figure 1. The air supply to the jets is first dried and then stored in a 1.8 cubic meter supply tank. Flow straightening and turbulence reduction is performed in a 15 cm diameter by 50 cm length section immediately upstream of the nozzle contraction. The flow management section consists of a 5 cm length of acoustic foam followed by several perforated plates, a 7.6 cm length of packed straws and 6 fine screens. A pressure regulator and throttling valve located upstream of the flow management section were used to control the stagnation pressure of the jet.

A cubic contoured contraction connects this section to the nozzle. An axisymmetric supersonic nozzle with an exit diamter of 10 mm was used for these experiments. The nozzle contour was designed using the method of characteristics with a computer program provided by Mr. Charles Johnson of the NASA-Langley Research Center. The inviscid design Mach number of the nozzle was 2.0. The nozzle contour design also

included a boundary layer correction. This correction was calculated for an average Reynolds number of 20,000 since the nozzle was intended for use at both lower and higher Reynolds number conditions.

The jet exhausts into a low pressure anechoic test chamber of dimensions 1.1 m x .76 m x .71 m. The chamber is lined with a 5 cm thick layer of Scott Pyrell acoustical foam. The foam absorbs 90% of the incident noise for frequencies above one kilohertz. A schematic diagram of the test chamber is shown is Figure 2.

An electric drive system capable of translating in three dimensions with a rotational stage in the horizontal plane is used to position the sensor probes. The probes used in this study consisted of Pitot and static pressure probes, normal hot-wire probes and 1/8-inch condenser microphones. The flow probes are mounted on slender brass wedges. An example is shown in full scale in Figure 3.

The pressure in the chamber was controlled by adjusting a variable throat diffuser located on the outlet side of the test chamber. The low pressure in the chamber was maintained by a 0.1 m^3/sec displacement Kinney vaccuum pump. The pump is isolated from the test facility by a 30 cubic meter tank and by a section of flexible pipe.

A glow discharge device was used to artificially excite the jet. A device of this type had previously been used by Kendall (32) to excite a supersonic boundary layer. The excitation device was mounted within 2 mm of the nozzle exit.

The discharge device consists of a 1 mm diameter tungsten rod insulated by a ceramic sleeve and held in the nozzle wall by a press fit brass outer sleeve. The glow discharge was produced between the tungsten and the brass by applying a large negative potential (-400 V) to the tungsten rod. The discharge was then oscillated at a selected frequency using an audio generator and a power amplifier.

B. Instrumentation

Pressure measurements were made with a mercury manometer referenced to a vaccuum of 30 micrometers of mercury. A pressure tap was located in the flow management section upstream of the nozzle for measuring the jet stagnation pressure and a static pressure tap was mounted near the nozzle exit. Chamber pressure taps were also located on the top wall of the facility. The stagnation temperature upstream of the nozzle was monitored using an iron-constantan thermocouple.

Both a Pitot probe and a static pressure probe were used in this study. The Pitot probe consists of a 0.53 mm outside diameter tube with a flat end cut perpendicular to the tube axis. Matthews (33) calibrated a probe of this type and found the viscous correction to the measured pressure to be negligible for flows in the Reynolds number range of this study. In supersonic flow the Pitot probe is assumed to measure the stagnation pressure behind a normal shock. The static pressure probe consisted of a slender cone mounted to

the flat end of a 0.88 mm O.D. tube, Behrens (34) calibrated a probe of this type and from his results it was determined that the viscous correction was negligible at the Reynolds number of this study.

The normal hot-wire probes used in this study were DISA 55A53 subminiature probes mounted on brass wedges. From time to time, wires would break and replacement 5 micron diameter platinum plated tungsten wires were soldered to the probe supports. The associated constant temperature hot-wire anemometry electronics consisted of a DISA 55M01 main frame with a 55M10 standard bridge. The frequency response of the hot-wire and associated electronics was assumed to be flat within ±3dB for frequencies up to 60 kHz based on square wave response tests.

A Bruel and Kjaer 3.175 mm diameter type 4138 condenser microphone was used for the acoustic measurements. Based on factory specifications, the microphone was assumed to have omni-directional response ±3dB for angles $\pm 90^{o}$ to the microphone axis and for frequencies up to 60 kHz. Calibration of the microphones was done with a B & K type 4220 piston phone. Associated microphone electronics included a B & K type 2618 preamplifier and a B & K type 2804 power supply.

Frequency spectra of the microphone and hot-wire signals were made using a Tektronix 7L5 spectrum analyzer. For the present research a resolution window of 3 kHz and a sweep speed of .05 sec/kHz were used for spectral studies. A Saicor model SAI 43A correlation and probability analyzer was

used for correlating and phase averaging hot-wire signals. Taped records of sensor signals for later reduction were made using an Ampex FR 1300 tape recorder.

CHAPTER III

EXPERIMENTAL PROCEDURES

A. General

All of the measurements reported in this study were conducted on a nearly perfectly expanded ($P_n = P_{CH} \pm 0.5$ mm Hg) nominal M = 2 supersonic jet. The Reynolds number of the majority of the measurements reported was approximately 70,000. The stagnation temperature of the jet was room temperature which was approximately 294 K. A diagram of the coordinate systems used for the various measurements is shown in Figure 4.

Since the low frequency noise (below 1 kHz) was not absorbed by the acoustic tile, the microphone output was high pass filtered at 1.5 kHz (St = 0.028). The microphone output was also low passed at 70 kHz (St = 1.32) to remove a 100 kHz resonance associated with the response of this type of microphone in low ambient pressure conditions. For consistency the fluctuating portion of the hot-wire signal was also filtered at these frequencies.

B. Phase Averaging

The fluctuating signal from a probe at a position in a turbulent flow can be mathematically represented by

$$f(t) = \overline{f} + \tilde{f}(t) + f''(t)$$

where $\overline{f}$ is the mean (time-averaged) contribution, $\tilde{f}$ is the organized wave, and f'' corresponds to the random turbulent motion.

Conventional time averaging of f determines $\overline{f}$. The phase average of f is given by

$$\langle f(t) \rangle = \lim_{N \to \infty} \frac{1}{N} \sum_{n=0}^{N} f(t + n\tau)$$

where τ is the period of the wave-like disturbance and N is the number of cycles of the disturbance over which the phase average is taken. Since the turbulent portion of the signal is random, it averages to zero leaving

$$\langle f(t) \rangle = \overline{f} + \tilde{f}(t).$$

If the mean is subtracted from this equation, only the portion of the fluctuating signal generated by the periodic disturbances remains.

In order to phase average experimental signals effectively, a triggering signal must be supplied which is in phase with the periodic disturbance. One way of supplying this trigger is to use the triggering signal as the initiation of the experimental event being measured. In the case of the present measurements, this method was followed by

using the signal driving the artificial exciter to produce the phase averaging trigger.

For the present measurements an oscillating glow discharge was used to initiate the periodic disturbance. The rms fluctuating electrical power input to the discharge was calculated to be approximately 1×10^{-5} of the total energy flux of the jet.

C. Hot-wire Fluctuation Data Analysis

The instantaneous voltage fluctuation measured from a hot-wire probe in supersonic flow can be represented mathematically by the following expression (35):

$$\frac{e'}{\overline{e}} = Am \frac{(\rho u)'}{\overline{\rho u}} + A_T \frac{T_t'}{\overline{T_t}}$$

For the hot-wire measurements reported in this study, since the stagnation temperature of the jet is approximately equal to the ambient temperature in the test chamber, it was normally assumed that stagnation temperature fluctuations were negligible. This assumption implies that the voltage fluctuations are proportional to mass velocity fluctuations. This proportionality factor, Am, was determined from direct calibration of each hot-wire probe where

$$Am = \frac{\partial \ln \overline{e}}{\partial \ln \overline{\rho u}} \Bigg]_{T_w,\ T_t}$$

The calibration was performed by locating the hot-wire probe on the centerline of the jet near the nozzle exit and varying local $\overline{\rho u}$ by adjusting the upstream stagnation pressure. Measurements of $\overline{e}$ were then made with T_t and T_w held constant. Values of Am were found to be negligibly affected by changes in overheat and to be primarily a function of mean $\overline{\rho u}$. This result is similar to findings observed by Rose in a supersonic boundary layer study (36).

The assumption of negligible T_t fluctuations was checked by performing a complete modal decomposition of the hot-wire voltage output for both natural and excited jet measurements. The methods of Ko et al (37) and Rose (36) were followed for reducing this data. From the results of the modal decompositions it was found that T_t fluctuations were responsible for less than 2% of the hot-wire rms voltage fluctuations for all typical experimental situations checked. This finding thus justified the neglection of T_t fluctuations in the hot-wire data reduction for the purpose of this study.

CHAPTER IV

EXPERIMENTAL RESULTS

A. Natural Jet

A.1. Mean Flow Field

Centerline Mach numbers for the Re=70,000 jet are shown in Figure 5. The Mach numbers are calculated from Pitot and static pressure measurements using standard compressible flow relationships. The average centerline Mach number from x/D = 1 to x/D = 8 was found to be 2.12 with variations of ±4% due to the weak shock cell structure of the jet. These measurements indicate the potential core length of the jet to be between 8 and 10 diameters. The sonic point in the jet is reached between 18 and 20 diameters downstream of the nozzle exit. These mean flow results are quite similar to the results obtained by Dutt (20) for a M = 2.0, Re = 2.6 x 10^6 cold air jet, and also similar to low Reynolds number, Re = 7900, measurements by Morrison (30) in a M = 2.1 jet.

Radial Mach number profiles for x/D = 1, 5, 10 and 15 are shown in Figure 6. These measurements show that the mean flow changes from a profile with a central region of uniform velocity to an approximately Gaussian profile by x/D = 10.

A.2. Fluctuating Flow Field

Frequency spectra of the hot-wire fluctuation signal obtained from the radial position of maximum voltage fluctuation (which is approximately the center of the jet shear layer) are shown in Figure 7 for several x/D locations. Beyond x/D = 8 the probe was located on the centerline of the jet. These spectra show that high frequency flow fluctuations centered around a Strouhal number of approximately 0.6 grow rapidly and dominant the spectra for the first three diameters downstream of the jet exit. At x/D = 4 although the high frequency fluctuations still dominate the spectra a marked increase in the amplitude of low frequencies (below St = 0.25) can be seen. From x/D = 4 to x/D = 6 the high frequency fluctuations steadily decay, transfering energy into intermediate frequencies around St = 0.30.

Spectral energy transfer to intermediate frequencies continues from x/D = 6 to x/D = 8 resulting in a fully developed turbulent spectrum at x/D = 8. Beyond x/D = 8 the fluctuation spectra continuously shift towards lower frequency content with downstream location as indicated by the spectrum at x/D = 10. The development of these spectra is quite similar to spectra measured by Miksad (38) in an incompressible free shear layer.

These spectra differ considerably from the low Reynolds number spectra (30) which were found to be dominated by a narrow frequency band near St = 0.2 for the first 10 jet diameters.

Figure 8 shows radial profiles of the total mass velocity fluctuations in the jet for several downstream positions. The measurements are reported in terms of rms mass velocity fluctuations, $(\rho u)_{rms}$, non-dimensionalized by the mean mass velocity $(\overline{\rho u})_o$ at the centerline of the nozzle exit. The radial peak of the fluctuation amplitude moves toward the center of the jet and the width of the shear layer increases with downstream location. By x/D = 9 it is apparent that large amplitude fluctuations have reached the jet centerline indicating the end of the potential core region. This result is consistent with the centerline Mach number measurements which showed a decrease in Mach number beginning near x/D = 9.

Flow fluctuation amplitude measurements as a function of x/D are shown in Figure 9. These measurements were obtained with the hot-wire located in the center of the shear layer until the end of the potential core where the hot-wire was moved to the jet centerline. The measurements show that the amplitude of the wide band-passed fluctuations grows exponentially for the first 3 downstream diameters. The amplitude of the fluctuations then oscillated from x/D = 4 to x/D = 7 before beginning a steady decline at x/D = 8. Also shown in the figure for comparison are measurements obtained by Morrison (30) in the low Reynolds number jet. An obvious increase in the growth rate of the total fluctuations as well as a shift in the axial position where the fluctuation amplitudes saturate is apparent between the two Reynolds number conditions. However, the peak fluctuation

amplitude is identical for the two jets within the experimental uncertainty.

Amplitude measurements of band-passed components of the hot-wire signal in the jet shear layer are shown in Figure 10. A 24 dB/Octave filter was used to obtain these measurements with cut off frequencies of ±20% around the center frequency of interest. All of the measured components grow at a constant exponential rate for the first 2½ to 3 downstream diameters with the higher frequency fluctuations growing faster.

Assuming this initial region of fluctuation growth to be governed by classical linear stability theory the mathematical representation for the fluctuating flow properties is given by

$$q = q(r)e^{-k_i x}\, e^{(k_r x + n\theta - \omega t)}$$

For a parallel flow M = 2.0 jet Tam (21) has obtained the relationship for k_i, the axial growth rate as a function of angular frequency ω. A non-dimensional graph of Tam's predictions with the present data is shown in Figure 11. The trend of the experimental growth rates, increasing growth rate with increasing Strouhal number, agrees with Tam's theoretical prediction. Moreover, the experimental growth rates and theoretical values are quite close for the two intermediate Strouhal numbers. Beyond x/D = 2½ after the high frequency fluctuations have grown to approximately 3% of the mean exit mass-velocity non-linear flow fluctuation

effects become apparent. These effects show up in the decreasing growth rates of the two higher frequencies and in increasing growth rates at the lower frequencies.

Between x/D = 3½ and x/D = 5½ the amplitude of the St = 0.094, St = 0.19, and St = 0.76 components saturate and then oscillate. The St = 0.38 component however goes through a region of slow growth between x/D = 3½ and 5½. This region of secondary growth for intermediate frequencies was also observed in the spectral results. Beyond x/D = 9 all frequencies show a continual decline in amplitude. The beginning of this region occurs approximately at the end of the potential core region as indicated by the mean flow measurements.

A.3. Acoustic Measurements

Sound pressure level (SPL) contours of the overall near field noise are shown in Figure 12. Since the measurements were made in a low pressure facility, the reference pressure used to calculate the dB level was scaled by the ratio of the chamber pressure to standard atmospheric pressure. The equation used to calculate SPL is given by

$$SPL = 20 \log \left[P_{rms} / [P_{ref} \ (P_c/P_{atm})] \right], \quad P_{ref} = 2 \times 10^{-5} \ \frac{\text{dynes}}{\text{cm}^2}$$

The near field contours are similar to high Reynolds number measurements in amplitude levels and general shape of the contours (39). The contours are also similar in shape and amplitude to the noise contours Morrison (30) measured in his

low Reynolds number study at the same Mach number. (The low Reynolds number contours are shown in dashed lines on the figure.) However, one important difference between the low Reynolds number results and the present measurements is obvious. The low Reynolds number contours are displaced downstream 6 to 10 jet diameters from the high Reynolds number contours. This displacement is most probably related to the fact that the flow fluctuation amplitudes saturate further downstream in the low Reynolds number jet. This feature seems to have important implications with regard to the noise production mechanism proposed by Morrison (30). A discussion on this subject will be presented in the Natural Jet Measurements summary section.

Figure 13 shows a SPL directivity plot of the overall noise from the jet. Also shown on this figure are extrapolated data from experiments by Dosanjh and Yu (40) of a M = 2.0 jet exhausting to atmosphere pressure (Re = 1.2×10^6). An important difference in generating these plots should be noted. The Dosanjh and Yu data were generated by moving the microphone on an arc of 180 jet diameters centered at the nozzle exit.* Due to size limitations of the present facility, the moderate Reynolds number measurements were made with an arc of 24 jet diameters.

---

*The Dosanjh and Yu data were extrapolated to the 24 jet diameter arc by assuming a (1/R) dependence in the sound pressure amplitude.

The high Reynolds number curve exhibits less directivity than the moderate Reynolds number measurements. This effect is probably at least partly due to the large difference in arc lengths used for obtaining the data. However, both curves do show that the highest levels of noise produced by the jets propagate at angles less than 45^{o} to the jet axis.

Spectral analysis of the microphone signal obtained at several locations along a constant radial coordinate are presented in Figure 14. These spectra show a shift towards increased lower frequency content as downstream position is increased. This trend has been noted in high Reynolds number jet noise measurements by a number of investigators (19, 27). This trend is also in general agreement with the hot-wire spectral results mentioned earlier.

To demonstrate the effect of Reynolds number on the noise frequency content, spectra from three different jets are presented in Figure 15. These spectra were measured near the regions of major noise production of the three jets. The bottom spectrum is from Morrison's low Reynolds number jet, the middle spectrum is from the present measurements, and the top spectrum was reported by Laufer et al. (19) for a Re = 2.6×10^{6}, M = 1.97 jet. At the low Reynolds number condition, the flow is dominated by a narrow band of frequencies and the noise is also relatively narrow banded. At the two higher Reynolds number conditions, the spectra are quite full, however, both have a broad peak around St = 0.2 which coincides with the low Reynolds number peak.

SPL contours of the near field noise band passed around three different spectral components (St = 0.094, St = 0.19 and St = 0.38) are shown in Figure 16. These frequencies encompass a large portion of the broad peak of the major noise production spectrum. Two important general features of these contours should be noted. One is the downstream lobes which are apparent at all three frequencies. The other feature is a bulge located in the upstream region of the contours. This upstream bulge is barely apparent in the highest Strouhal number contours, but becomes more obvious in the lower Strouhal number plots. For the lowest Strouhal number contours, a definite separation between the two regions is evident. These two regions have been noticed before by prior investigators (21, 27).

Figure 17 shows SPL directivity plots for four Strouhal number components. These plots were generated using an arc length of 24 diameters. A constant bandwidth of 3 kHz centered on the measured frequency was used for obtaining this data. A consistent decrease in the dominant noise radiation angle with decreasing frequency is apparent. This feature has also been noted in high Reynolds number jets (19, 27). It should also be pointed out that the highest sound pressure levels were attained by the two intermediate Strouhal numbers.

A.4. Summary of Natural Jet Results

The mean flow measurements show that the jet has an initial central region of uniform velocity which transitions to an approximately Gaussian profile by x/D = 10. The average Mach number of the jet was found to be 2.12 in the potential core region and the sonic point was reached between 18 and 20 diameters downstream. These mean flow results are similar to both high and low Reynolds number measurements of previous investigators.

The flow fluctuation measurements demonstrate that high frequency fluctuations grow at a constant exponential rate for the first 2½ to 3 downstream diameters. Beyond x/D = 3 non-linear effects become apparent and by x/D = 5, the flow fluctuation spectra are quite broad and the total fluctuation amplitude attains a saturated condition. By x/D = 8 the spectra have become fully developed. Beyond x/D = 8 the amplitude of the flow fluctuations decreases, and the spectral content of the fluctuations shifts progressively to lower frequencies.

These results differ considerably from low Reynolds number measurements at the same Mach number (30). The lower Reynolds number fluctuations were found to be dominated by a narrow band of frequencies near St = 0.2 for the first 10 diameters downstream of the jet exit. Growth rates of the flow fluctuations in the low Reynolds number jet are much slower and the fluctuation level does not saturate until x/D = 10.

Acoustic spectra demonstrate that the noise produced by the moderate Reynolds number jet has a broad frequency content. The content of the acoustic spectra was observed to move to lower frequencies as the microphone was moved downstream.

SPL contours of the overall acoustic field were found to be similar in shape and amplitude to both low and high Reynolds number measurements. However, the low Reynolds number contours are displaced by approximately 6 to 10 jet diameters downstream. This displacement was attributed to the observed shift in the location of the amplitude saturation region of the flow fluctuations. Since apparently the major effect of changing the total flow fluctuation growth rate upon the noise contours was simply to shift the contours axially and not to change their shape or amplitude significantly, it can be inferred that the major noise production mechanism is largely independent of fluctuation growth rate. It seems more plausible in light of these results to suppose that the major noise generation mechanisms may be characteristic of phenomena which occur downstream of the initial region of unstable fluctuation growth.

Morrison (30) postulated that the rapid growth and decay of the instability in the jet is the dominant noise production mechanism. The observations in this study indicate that the decay of individual spectral components is of more importance in noise generation. This agrees in concept with the instability 'cut-off' mechanism discussed by Liu (24).

Acoustic results also indicate that two localized regions of major noise production are present in the acoustic field of the jet. This feature has been noted previously in a number of high Reynolds number investigations. It was also noted that the angle with respect to the jet axis of the dominant noise radiation decreased with decreasing frequency. This result had also been noted by several investigators of high Reynolds number jet noise.

B. Artificially Excited Jet

B.1. Effects of Excitation

B.1.a. The Flow Field. In order to develop an understanding of the nature of the coherent fluctuations within the jet, an artificial disturbance was input at the nozzle exit using a glow discharge. Figure 18 shows an example of the frequency spectra at several downstream locations in the center of the shear layer with the jet excited at St = 0.38.

The spectra show that the exciter generates a disturbance concentrated at the fundamental forcing frequency and its first harmonic. Over the first six downstream diameters the fundamental steadily grows while the first harmonic decays. At x/D = 6 the amplitude of the fundamental saturates as the harmonic disappears. Beyond x/D = 6 the fundamental rapidly decays until by x/D = 10 the fundamental's presence is barely distinguishable from the background fluctuations.

Although the input disturbance from the exciter dominates the flow fluctuation spectra near the nozzle, its effect is initially localized within the thin shear layer of the jet. This fact can be seen in Figure 19 which shows a radial profile of the total mass velocity fluctuations at x/D = 1 for a jet excited at St = 0.19.

The effect of the excitation on the jet centerline mass-velocity fluctuations for four excitation frequencies is shown in Figure 20. These measurements were bandpass filtered ±1 kHz around the excitation frequency. An interesting result is evident from this figure. Apparently the jet core is much more responsive to excitation at the intermediate frequencies of St = 0.19 and St = 0.38. This result is closely analogous to results obtained by Crow and Champagne (11) in a turbulent subsonic jet which was found to be most responsive to a St = 0.3 excitation. The exact mechanism by which the jet selects these frequencies is still poorly understood but it apparently exists in both subsonic and supersonic jets.

The effect of the excitation on the mean flow can be seen in Figures 21 and 22. Figure 21 shows radial profiles of mean $\overline{\rho u}$ for a jet excited at St = 0.19. For comparison mean $\overline{\rho u}$ profiles for a natural jet are shown in Figure 22. These figures show that the artificial input disturbance causes the jet potential core region to end nearer the nozzle exit than in the natural jet. This effect can be seen more clearly in Figure 23 which shows that the centerline $\overline{\rho u}$

begins a steady decrease at approximately x/D = 6 for the excited jet as compared to x/D = 8 for the natural jet.

B.1.b. The Acoustic Field. SPL contours of the overall near field noise for the jet excited at St = 0.19 are shown in Figure 24. The shapes and positions of these contours are approximately the same as the natural jet contours shown in Figure 12. However, an increase in the noise level at corresponding locations in the acoustic field is apparent.

A directivity plot generated from these contours is shown in Figure 25. For comparison the natural jet measurements are also shown on the plot. This plot shows that the directivity of the noise radiation in the two cases is almost identical although the amplitude is approximately 2 to 3 db higher in the excited case.

Spectra of the acoustic radiation from a jet excited at St = 0.19 are shown in Figure 26 for several x/D locations at a constant radial location. Upstream of x/D = 8, little effect from the excitation disturbance is observed. However, from x/D = 8 downstream discrete peaks are seen in the spectra at the fundamental forcing frequency and its higher harmonics. The strength in these peaks shifts steadily toward the lower harmonics and the fundamental as downstream position is increased. This shift is analogous to the shift in the natural spectra towards lower frequencies with increased downstream location.

SPL contours filtered around the fundamental excitation frequency are shown in Figures 27 a, b, and c for St = 0.094, St = 0.19, and St = 0.38. If the plots of the low St number contours are compared to the natural contours, little change is apparent in the upstream bulge area. However, the downstream region of maximum noise emission has been pushed farther from the jet and is beyond the limits of the probe drive. Fortunately, the lobed portions of the two higher Strouhal number contours were within the probe drive range. Both of the higher Strouhal number plots show a considerable amplitude increase over the natural case in the SPL of the downstream lobes. However, there is little indication of the upstream bulge area which was apparent in the natural contours in the St = 0.19 case.

SPL directivity plots filtered around St = 0.19 and St = 0.38 are shown in Figures 28 a and b for both excited and nonexcited jets. As would be expected due to the concentrated nature of the excited acoustic spectra, there is a considerable increase in the SPL for a given angle. However, surprisingly there seems to be very little change in the directivity of the noise radiation. This result implies that the artificial disturbance generates noise by the same mechanism responsible for the downstream noise emission pattern in the natural jet. This implication makes it of considerable interest to determine some of the important characteristics of the artificially excited disturbance and its noise radiation.

B.2. Excited Flow Disturbance Measurements

B.2.a. Phase Measurements. Measurements of the axial wavelength of excited disturbances in the jet were made by cross-correlating the hot-wire signal with the exciter and measuring the change in the time lag of the peak of the correlation curves for various downstream positions. An example of these measurements for a typical disturbance is shown in Figure 29.

The results of the wavelength measurements, presented in terms of non-dimensional wave number k_r as a function of disturbance Strouhal number, are shown in Figure 30. These measurements show an approximately linear relationship between k_r and St. This type of relation was predicted by Tam in an early stability study of the supersonic jet (21) and has been measured in subsonic jets by Chan (23). Tam's prediction for a spiral mode instability ($n = \pm 1$) in a $M = 2.1$ jet is shown in Figure 30. The fact that Tam's predicted values are somewhat lower in terms of wavenumber should not be viewed too critically, since he used a simple non-diverging mean flow profile in his stability model.

Multiplying the axial wavelength by the frequency of the disturbance gives the axial phase velocity of the disturbances. Figure 31 shows the axial phase velocity as a function of Strouhal number. The trend of increasing velocity with Strouhal number for low frequency disturbances was also noted by Chan (23) for azimuthal modes $n = 1$ and $n = 2$ in a subsonic jet.

It is notable that the average convection velocity for disturbances between St = 0.28 and St = 0.48 is approximately 0.80 U_o. This value compares closely to the convection velocity of 0.83 U_o measured by Dutt from laser cross-correlations in a high Reynolds number supersonic jet for a St = 0.4 disturbance.

An important point to note in addition is that disturbances traveling faster than 0.65 U_o will be traveling supersonically with respect to the air outside the jet. This point is important because Tam (22, 26) predicts that only waves with supersonic phase velocities will radiate sound by his noise generation mechanism. Observing Figure 31, it can be noted that the St = 0.094 disturbance travels at a subsonic phase speed. However, both natural and excited noise contours show that this mode radiates a considerable amount of noise. Previous low Reynolds number measurements at Oklahoma State University (28-30) have also noted the fact that disturbances convecting downstream subsonically can produce noise. Morris and Tam (26) attribute this possibility to the amplitude variation of the disturbances, which can cause even a subsonic disturbance to have a significant portion of supersonic phase components.

B.2.b. Amplitude Measurements. Figure 32 shows the level of the coherent disturbance mass velocity fluctuations in the jet shear layer as a function of downstream position for the two excitation frequency components shown to have

the most effect on the jet core. These data were produced by filtering the hot-wire signal around the excitation frequency and then phase averaging the bandpassed signal. The measurement location in the shear layer was chosen at the position of maximum bandpassed hot-wire voltage fluctuation level. The coherent amplitude level of both frequencies develop in a similar manner with the higher frequency disturbance development shifted upstream approximately 2 to 3 diameters. It should be noted that the coherent fluctuation amplitudes decay at a much faster rate than the bandpassed natural fluctuation levels shown in Figure 10. The fast decay of the coherent fluctuation has been postulated by Liu (24) as an important noise generation mechanism.

According to Tam (22) the total coherent energy flux of the jet is an important measure of its noise generation strength. Tam's full expression for the total coherent fluctuation energy is given by

$$E_t = \int_0^\infty \left[\bar{\rho}\, \bar{u}\, (\tilde{E}_{K.E.}) + \frac{\bar{u}}{2\gamma p_{ch}} (\tilde{p}^2) + \tilde{p}u \right] r\,dr \quad \text{where}$$

$$\tilde{E}_{K.E.} = \tfrac{1}{2} (\tilde{u}^2 + \tilde{v}^2 + \tilde{w}^2)$$

It was experimentally impractical to measure all the terms in the integral, however, an attempt was made to measure the axial velocity kinetic energy portion of the integrand. To determine the integrated energy to this approximation, several radial measurements were made at each x/D location

for the St = 0.19 disturbance. The experimental measurements were then integrated numerically to evaluate the coherent energy for each axial position. The results of the measurements are compared to Tam's prediction in Figure 33. Reasonable agreement between the trend of the measured values and theory are found over the growth region of the function. The fact that the experimental values are somewhat lower than theory should be expected since the measurements only account for a portion of the integrand. On the decay side of the curve, however, the experimental values seem to damp at a considerably faster rate than Tam's prediction. Assuming that the measured portion of the integrand represents a constant fraction of the total integrand the faster decay of the measured values may represent a significant departure from the theory. The reason for this departure might be due to the fact that Tam considers only damping due to mean profile changes whereas in the experimental case non-linear effects also contribute to the fluctuation decay.

B.3. Acoustic Radiation from Artificially Excited Disturbances

B.3.a. Amplitude Measurements. By phase averaging the microphone signal in the noise radiation field, the fraction of the total signal directly caused by the excited flow disturbances was determined. Figure 34 shows the percentage of the phase averaged component as a function of downstream position for three excitation frequencies (St = 0.094, 0.19,

0.38). These measurements were recorded at a constant radial location of 8 diameters. At low values of x/D, the noise at all three Strouhal numbers shows a low percentage of the phase averaged component. However, at approximately x/D = 8, both the two higher Strouhal numbers show an increase in phase averaged components. The St = 0.38 phase averaged component goes above 50% by x/D = 12, while the St = 0.19 component reaches this value slightly farther downstream at x/D = 16. These points correspond approximately to the location of the inflection region in the filtered natural jet contours (Figure 16) indicating the beginning of the downstream lobed area. The St = 0.094 component also follows this trend showing an increase in its phase averaged percentage around x/D = 24, which also corresponds to the beginning of the lobed area in the filtered natural contours; although its maximum percentage of phase averaged component is considerably lower than the two higher frequency components.

In agreement with these results several investigators of high speed jets (20, 41, 42) have also noted high correlations for the noise at small spherical angles ($\beta \leq 45^{o}$).

B.3.b. Phase Measurements. Measurements of the wavelengths of the acoustic radiation in the radial and axial directions were obtained for two excitation Strouhal numbers (St = 0.19 and St = 0.38). These measurements were made by cross-correlating the microphone signal with the exciter signal and measuring the time lag change for various positions

in the acoustic field in a similar fashion to the flow wavelength measurements. The axial and radial wavelengths were used to calculate the acoustic wavelength normal to the wave fronts. Table I shows the results of these measurements for various locations in the acoustic field. Also included in the table are the calculated angle, α, of the wave propagation with respect to the jet axis and the corresponding calculated Mach wave angle, μ, of the supersonic flow disturbance. A schematic depicting the relationship of the flow and acoustic wave lengths is shown in Figure 35. The acoustic phase speed, C_a, was calculated from the measured acoustic wavelength and the frequency. This speed is compared to the acoustic velocity calculated from the standard compressible flow relation $a_o = \sqrt{\gamma R_g T_o}$. This comparison gives an indication of the measurement error.

It can be seen from the table that the faster flow disturbance (St = 0.38), produces acoustic waves propagating close to the Mach angle computed from the disturbance speed. The slower disturbance (St = 0.19), however, produces waves which are inclined at an angle considerably lower than the predicted Mach angle. This feature was also observed by Morrison (30) in his low Reynolds number measurements for waves traveling just above the speed of sound.

Based on these results and Morrison's measurements, it seems that a simple eddy Mach wave model for the major noise generation mechanism is not of sufficient complexity to

explain all of the measured noise field properties. However, it does appear that a Mach wave type of noise radiation does occur for higher frequency disturbances.

Mach wave type radiation has been noticed by a number of experimenters using flow visualization techniques (17, 18). Recently Dutt (20) found that the angle of the Mach waves in his shadowgraphs implied a disturbance convection velocity which was in agreement with his Laser cross-correlation measurements.

To approximately locate the major noise sources in the jet, a simplified ray tracing technique was used. This technique involved drawing a line perpendicular to the acoustic wave front from a point approximately in the center of the contour lobes. The point of intersection of the perpendicular line with the jet then indicates the location of the major noise sources under the assumption that the noise propagates in a plane wave fashion.

The results of this technique indicate that the major noise sources for St = 0.38 noise radiation are located between 6 and 8 diameters downstream of the jet exit. The major noise sources for the St = 0.19 noise radiation were found to be located between 8 and 10 diameters downstream. Flow fluctuation amplitude measurements have shown that both of these locations are downstream of the initial growth of the flow disturbances, and in the axial region where the disturbances amplitude saturates and begins to decay.

This finding appears to support theoretical studies by Liu (24) where he attributed a strong noise generation mechanism to the non-linear disintegration of the coherent disturbance.

The azimuthal character of the acoustic radiation from excited disturbances at St = 0.19 and St = 0.38 was determined by measuring the phase relationship between the microphone and exciter signal for various angles of θ. These measurements were made at an axial location of x/D = 12 on an arc of radius r/D = 3. The amplitude of the phase averaged signal was also recorded for each measurement position. The results of the measurements are shown in Figures 36a and 36b. The amplitude measurements are non-dimensionalized by the amplitude of the maximum phase averaged signal on the arc. Numerical fits for the data were obtained by superposing three azimuthal modes of mode numbers n = 0, +1, and -1. (It is generally accepted that low mode numbers dominate axisymmetric flows.) These modes are mathematically represented by the equation

$$q_n = A_n e^{i(n\theta - \omega t + \alpha_n)}; \quad n = 0, +1, -1$$

where α_n was used to represent an arbitrary phase difference between modes. Before attempting to find A_n and α_n for each mode it was assumed the $A_1 = A_{-1}$ and that $\alpha_1 = \alpha_{-1}$. Since the mean flow is axisymmetric α_1 and α_{-1} can be set to any θ. For simplicity $\theta = 0$ was chosen. The best fits for the data were found to be $A_o/A_1 = 1.4$ with $\alpha_o = 130^o$ for the

St = 0.19 disturbance and $A_o/A_1 = 0.5$ with $\alpha_o = 90^o$ for the St = 0.38 data. The indication that disturbances occur in both axisymmetric and antisymmetric modes is in agreement with Dutt's (20) findings for a high Reynolds number M = 2.0 jet.

It is of interest to note that the antisymmetric excitation device is apparently capable of exciting both antisymmetric and axisymmetric flow disturbances. This finding indicates that the excitation device does not necessarily dictate the downstream character of the artificial disturbance. Consequently, this result encourages somewhat greater confidence to be placed in the applicability of the excited measurements to natural jet phenomona.

B.4. Summary of Excited Jet Results

It was found that the artificial exciter generates a flow disturbance at the fundamental forcing frequency and its higher harmonics. For several diameters downstream of the nozzle exit, it was observed that the flow fluctuation spectral content in the jet shear layer is concentrated at the excitation frequency and its harmonics. Farther downstream, the spectral content of the flow fluctuations disperse and the effect of the excitation on the flow spectra reduces until by x/D = 10 it is finally unobservable. Centerline flow fluctuation measurements demonstrated that the jet core was most responsive to excitation at the intermediate Strouhal numbers (St = 0.19 and St = 0.38). Also, excitation

at St = 0.19 caused the jet potential core region to end earlier than the nonexcited case.

The acoustic field spectra near the nozzle exit were not noticeably affected by the excitation. Farther downstream, near the SPL contour lobes, peaks in the acoustic spectra appear at the fundamental forcing frequency and its harmonics. The relative strength of these peaks shifts to the lower harmonics and fundamental as downstream position increases.

Noise amplitude measurements indicated that a large portion of the noise from the excited disturbances propagates toward the downstream lobed region of the contours. Phase averaged acoustic measurements confirmed this fact.

The directivity of the noise from the excited disturbance was found to be almost identical to the natural case for the two Strouhal numbers observed (St = 0.19 and St = 0.38). These measurements indicate that organized flow disturbances are directly responsible for a major portion of the noise radiation produced by supersonic jets.

Flow measurements of the excited disturbances demonstrated that the disturbance wavelength decreases approximately linearly with increasing Strouhal number; a trend predicted by Tam using a linear stability theory. Phase velocities calculated from the measured wavelengths show an increase in velocity at low Strouhal numbers. Above St = 0.38 up to St = 0.84, the phase velocity remains approximately constant with wave speeds between 0.76 U_o to 0.81 U_o.

Phase averaged amplitude measurements of excited flow fluctuations in the jet shear layer show that the St = 0.19 and the St = 0.38 disturbances peak in amplitude near x/D = 6 however the St = 0.38 disturbance decays at a considerably faster rate than the St = 0.19 disturbance in the region downstream of their peak. The amplitude of the integrated coherent energy flux of the St = 0.19 disturbance grew in reasonable agreement with Tam's theoretical prediction. However, the decay of the coherent energy flux occurred at a faster rate than predicted. This difference could be attributed to non-linear effects not included in Tam's theory.

Phase front measurements of the acoustic radiation indicated that the St = 0.38 disturbance radiates noise at approximately the Mach wave angle calculated from the phase velocity of the flow disturbance. The St = 0.19 disturbance radiates noise with wave fronts inclined at an angle considerably less than the Mach wave angle. This fact had also been noticed in low Reynolds number jets by Morrison (30).

By drawing a line perpendicular to the measured wave fronts at a point near the center of the acoustic lobes, the approximate location of the noise sources in the jet can be determined. The St = 0.38 noise source was found to be located between 6 and 8 diameters downstream of the nozzle exit. The St = 0.19 noise source was located between 8 and 10 diameters downstream of the nozzle exit. Both of these locations correspond to positions in the flow where the

amplitude of the fluctuations at these frequencies saturate and begin to decay.

Azimuthal acoustic measurements indicated that the noise radiation from the St = 0.19 and the St = 0.38 disturbances included both antisymmetric and axisymmetric modes. The lower frequency disturbance was found to contain a considerably larger portion of the axisymmetric mode than the higher frequency disturbance.

CHAPTER V

CONCLUSIONS

Flow and acoustic measurements were made on a M = 2.1 jet at a moderate Reynolds number of 70,000 in this study. The major goal of this research was to develop some experimental understanding of high speed turbulent jet noise production. The major results are listed as follows with the number of the figures supporting listed results given in parenthesis after each result.

A. Natural Jet

1. For the moderate Reynolds number jet, it was found that for the first 2½ to 3 diameters downstream of the nozzle exit high frequency flow instabilities dominate the shear layer fluctuations (Figures 7, 10).
2. By x/D = 4, the flow fluctuation amplitude has saturated and the spectral content cover a broad frequency range (Figures 7, 10).
3. Beyond x/D = 8, the spectral content consistently shifts to lower frequencies with increasing downstream position (Figure 7).

4. The mean flow of the moderate Reynolds number jet was similar to low Reynolds number (Re = 7,900) (30) and high Reynolds number measurements (Re = 2.6 x 10^6) (20) (Figures 5, 6).
5. Spectra of the noise radiated by the jet has a broad frequency content which also shifts to lower frequencies with increasing downstream position (Figure 14).
6. Comparisons of low and moderate Reynolds number SPL contours indicate that the growth rate of the flow fluctuations is not directly related to noise production (Figures 9, 12).
7. Two apparently distinct regions of noise production were found in the SPL contours; these regions were indicated by an upstream bulge in the SPL contours and a downstream lobed area (Figures 16 a, b).

B. Artificially Excited Jet

1. The artificial exciter generates a disturbance at the fundamental forcing frequency and its first harmonic which dominates the natural flow fluctuations in the jet shear layer for several diameters downstream of the nozzle exit (Figure 18).
2. The jet core was found to be most responsive to excitation at intermediate frequencies of St = 0.19 and St = 0.38 (Figure 20).

3. The wavelength of the artificial disturbances varies approximately linearly with Strouhal number, a trend predicted by Tam (21) (Figure 30).
4. The disturbance phase speed increases with increasing Strouhal number at low frequencies and then remains approximately constant (0.76 to 0.81) for Strouhal numbers 0.38 and above (Figure 31).
5. Phase averaged measurements of the flow fluctuations in the jet shear layer show that the St = 0.19 and St = 0.38 disturbance peak in amplitude near x/D = 6 with the higher frequency damping at a faster rate with downstream position (Figure 32).
6. The integrated coherent energy flux of the St = 0.19 disturbance grew in amplitude in reasonable agreement with Tam's theoretical prediction. However, its amplitude damps faster than Tam's prediction possibly due to non-linear effects not accounted for in the theory (Figure 33).
7. The noise from the excited disturbances is radiated predominantly towards the downstream lobed region of the noise contours with a directivity identical to the natural jet spectral components (Figures 28 a, b and 34).
8. Noise radiation from the St = 0.38 disturbance propagates near the computed Mach wave angle. Noise radiation from the St = 0.19 disturbance; however, does not propagate at the Mach wave angle (Table I).

9. A ray tracing technique indicated that the major noise production areas of the jet are in regions of flow where the disturbance amplitude has saturated and begun to decay.

10. The noise from the St = 0.19 and St = 0.38 disturbances occurs in both antisymmetric and axisymmetric modes (Figures 36 a, b).

BIBLIOGRAPHY

(1) Lighthill, M. J. "On Sound Generated Aerodymanically, I General Theory." Proc. Roy. Soc., A211 (1952), pp. 546-587.

(2) Lighthill, M. J. "On Sound Generated Aerodymanically, II Turbulence as a Source of Sound." Proc. Roy. Soc., A222 (1954), pp. 1-32.

(3) Ffowcs William, J. E. "The Noise From Turbulence Convected at High Speed." Phil. Trans. Roy. Soc., A255 (1963), p. 459.

(4) Phillips, O. M. "On the Generation of Sound by Supersonic Turbulent Shear Layer." J. Fluid Mech., Vol. 9 (1960), pp. 1-28.

(5) Ribner, H. S. "The Generation of Sound by Turbulent Jets." Advances in Applied Mechanics, Vol. 8 (1964), pp. 103-182.

(6) Pao, S. P. and M. V. Lowson. "Some Applications of Jet Noise Theory." AIAA Paper No. 70-233, 1970.

(7) Lilley, G. M., P. Morris, and B. J. Tester. "On the Theory of Jet Noise and its Applications." AIAA Paper No. 73-987, 1973.

(8) Doak, P. E. "Analysis of Internally Generated Sound in Continous Materials: 2. A Critical Review of the Conceptual Adequacy and Physical Scope of Existing Theories of Aerodynamic Noise, with Special Reference to Jet Noise." Journal of Sound and Vibration, Vol. 25 (1972), pp. 263-335.

(9) Brown, G., and Roshko, A. "The Effect of Density Difference on the Turbulent Mixing Layer." AGARD Conference on Turbulent Shear Flows. Conf. Proc. No. 93 (1971), p. 23.

(10) Winant, C. D., and F. K. Browand. "Vortex Pairing, the Mechanism of Turbulent Mixing Layer Growth at Moderate Reynolds Number." J. Fluid Mech., Vol. 63 (1974), pp. 237-256.

(11) Crow, S. C., and F. H. Champagne. "Orderly Structure in Jet Turbulence." J. Fluid Mech., Vol. 48 (1971), pp. 547-591.

(12) Lau, J. C., and M. J. Fisher. "The Vortex-Street Structure of 'Turbulent' Jets, Part 1." J. Fluid Mech., Vol. 67 (1975), pp. 299-337.

(13) Chan, Y. Y. "Noise Generated Wavelike Eddies in a Turbulent Jet." ICAS Paper No. 76-42, 1976.

(14) Mollo-Christensen, E. "Jet Noise and Shear Flow Instability Seen from an Experimenter's Viewpoint." J. Appl. Mech., Vol 34 (1967), pp. 1-7.

(15) Moore, C. J. "The Role of Shear-Layer Instability Waves in Jet Exhaust Noise." J. Fluid Mech., Vol. 80, Part 2 (1977), pp. 321-357.

(16) Bishop, K. A., J. E. Ffowcs Williams, and W. Smith. "On the Noise Sources of the Unsuppressed High-Speed Jet." J. Fluid Mech., Vol 50 (1971), pp. 21-31.

(17) Salant, R. F. "Investigation of Jet Noise Using Optical Holography." Department of Transportation Report No. DOT-TSC-OST-73-11, 1973.

(18) Lowson, M. V., and J. B. Ollerhead. "Visualization of Noise from Cold Supersonic Jets." J. Acoust. Soc. Am., Vol. 44 (1968), p. 624.

(19) Laufer, J., R. S. Schlinker, and R. E. Kaplan. "Experiments on Supersonic Jet Noise." AIAA Paper No. 75-478, 1975.

(20) Dutt, B. "Role of Large Scale Structures in the Noise Generation of a Turbulent Supersonic Jet." Ph.D. Dissertation, University of Southern California, 1977.

(21) Tam, C. K. W. "On the Noise of a Nearly Ideally Expanded Supersonic Jet." J. Fluid Mech., Vol. 51 (1972), pp. 69-95.

(22) Tam, C. K. W. "Supersonic Jet Noise Generated by Large Scale Disturbances." J. Sound and Vibration, Vol. 38 (1974), pp. 51-79.

(23) Chan, Y. Y. "Discrete Acoustic Radiation From a High-Speed Jet as a Singular Pertubation Problem." Canadian Aeronautics and Space Journal, Vol. 38 (1974), pp. 51-79.

(24) Liu, J. T. C. "Devloping Large-Scale Wavelike Eddies and the Near Jet Noise Field." J. Fluid Mech., Vol. 62 (1974), pp. 437-464.

(25) Morris, P. J. "Flow Characteristics of the Large-Scale Wave-like Structure of a Supersonic Round Jet." (Submitted for publication to the J. Sound and Vibration.)

(26) Morris, P. J. and Tam, C. K. W. "Near and Far Field Noise From Large-Scale Instabilities of Axisymmetric Jets." AIAA Paper No. 77-1351, 1977.

(27) Yu, J. C., and D. S. Dosanjh. "Noise Field of Supersonic Mach 1.5 Cold Model Jet." J. Acoust. Soc. Am., Vol. 51 (1973), pp. 1400-1410.

(28) McLaughlin, D. K., G. L. Morrison, and T. R. Troutt. "Experiments on the Instability Waves in a Supersonic Jet and Their Acoustic Radiation." J. Fluid Mech., Vol 69 (1976), pp. 73-95.

(29) McLaughlin, D. K., G. L. Morrison, and T. R. Troutt. "Reynolds Number Dependence in Supersonic Jet Noise." AIAA J., Vol. 15 (1977), pp. 526-532.

(30) Morrison, G. L. "Flow Instability and Acoustic Radiation Measurements of Low Reynolds Number Supersonic Jets." Ph.D. Dissertation, Oklahoma State University, Stillwater, Oklahoma, 1977.

(31) Stromberg, J. L. "Flow Field and Acoustic Measurements of Low Reynolds Number Transonic Jets." (M.S. Thesis, Oklahoma State University, Stillwater, Oklahoma, 1978)

(32) Kendall, J. M. "Supersonic Boundary Layer Stability Experiments." Proceedings of the Boundary Layer Transition Study Group Meeting, Vol. II, Aerospace Report No. TR-0158 (S3816-63)-1, 1967.

(33) Matthews, M. L. "An Experimental Investigation of Viscous Effects on Static and Impact Pressure Probes in Hypersonic Flow." Pasadena, CA: GALCIT, Hypersonic Research Project, Memo No. 44, 1958.

(34) Behrens, W. "Viscous Interaction Effect on a Static Pressure Probe at M = 6." AIAA J., Vol. 1 (1963), pp. 2364-2366.

(35) Kovasznay, L. S. G. "The Hot-Wire Anemometer in Supersonic Flow." J. Aero. Sci., Vol. 17, No. 9 (September, 1950), pp. 565-572.

(36) Rose, W. C. "The Behavior of a Compressible Turbulent Boundary Layer in a Shock-Wave-Induced Adverse Pressure Gradient." NASA TN D-7092, 1973.

(37) Ko, C. L., D. K. McLaughlin, and T. R. Troutt. "Improved Techniques for Hot-Wire Fluctuation Measurements in Supersonic Flows." AIAA Paper No. 76-398, 1976.

(38) Miksad, R. W. "Experiments on the Nonlinear Stages of Free-Shear-Layer Transition." J. Fluid Mech., Vol. 56 (1972), pp. 695-719.

(39) Howes, W. L. Callaghan, E. E., Coles, W. D., Mull, H. R., "Near Noise Field of a Jet-Engine Exhaust." NACA Report 1338, 1959.

(40) Dosanjh, D. S., and J. C. Yu. "Noise From Underexpanded Axisymmetric Jet Flow Using Radial Jet Flow Impingement." Proceedings, AFQSR-UTIAS Symposium on Aerodynamic Noise, Toronto, 1968, pp. 169-188.

(41) Dahan, P. C. and Elias, G. "Source Structure Pattern in a Hot Jet by Infrared-Michrophone Correlation." AIAA Paper No. 76-542, 1976.

(42) Maestrella, L. "Two Point Correlation of Sound Pressure in the Far Field of a Jet: Experiment." NASA TM-72835, 1976.

APPENDIX A

FIGURES

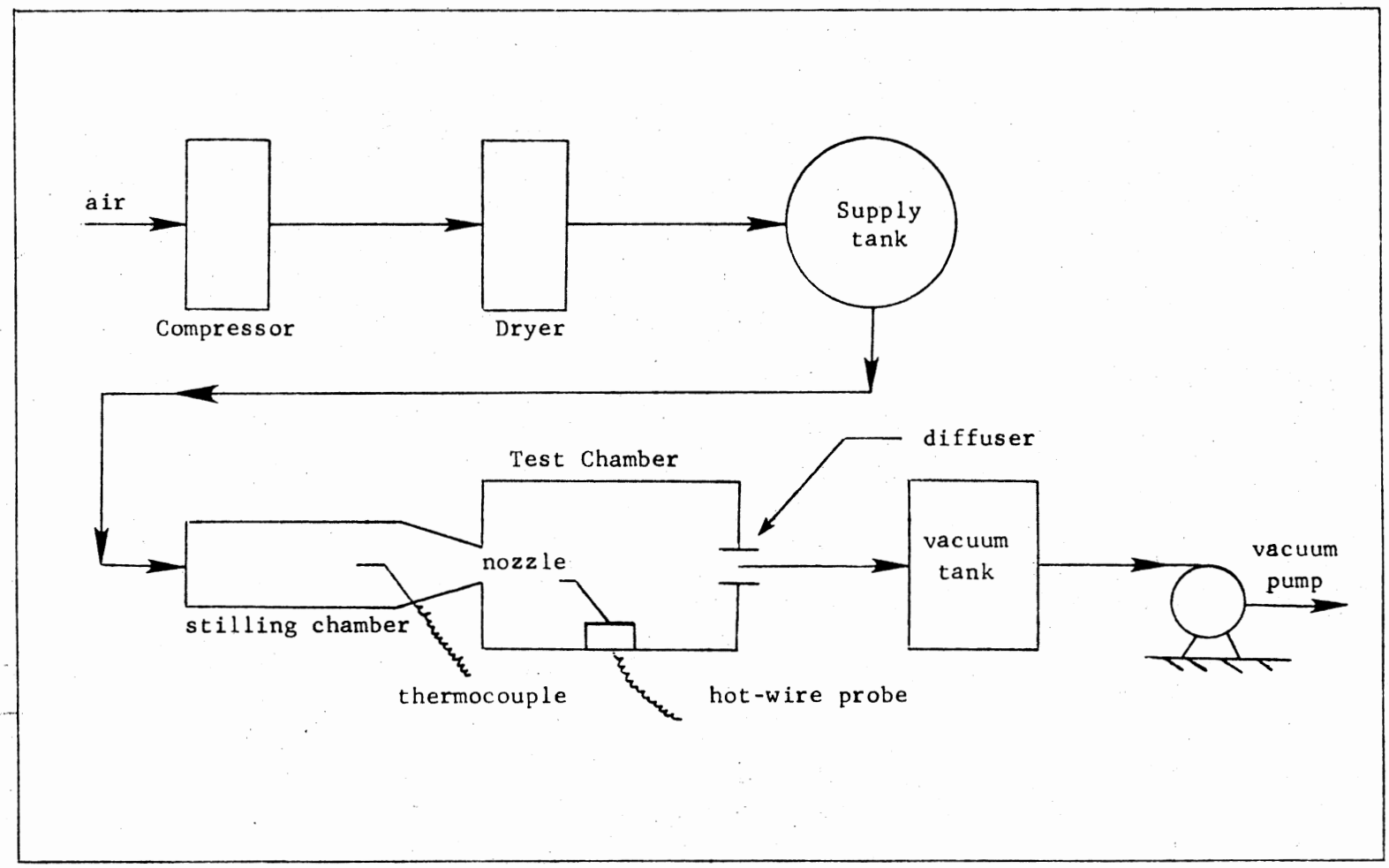

Figure 1. Schematic of Overall Facility

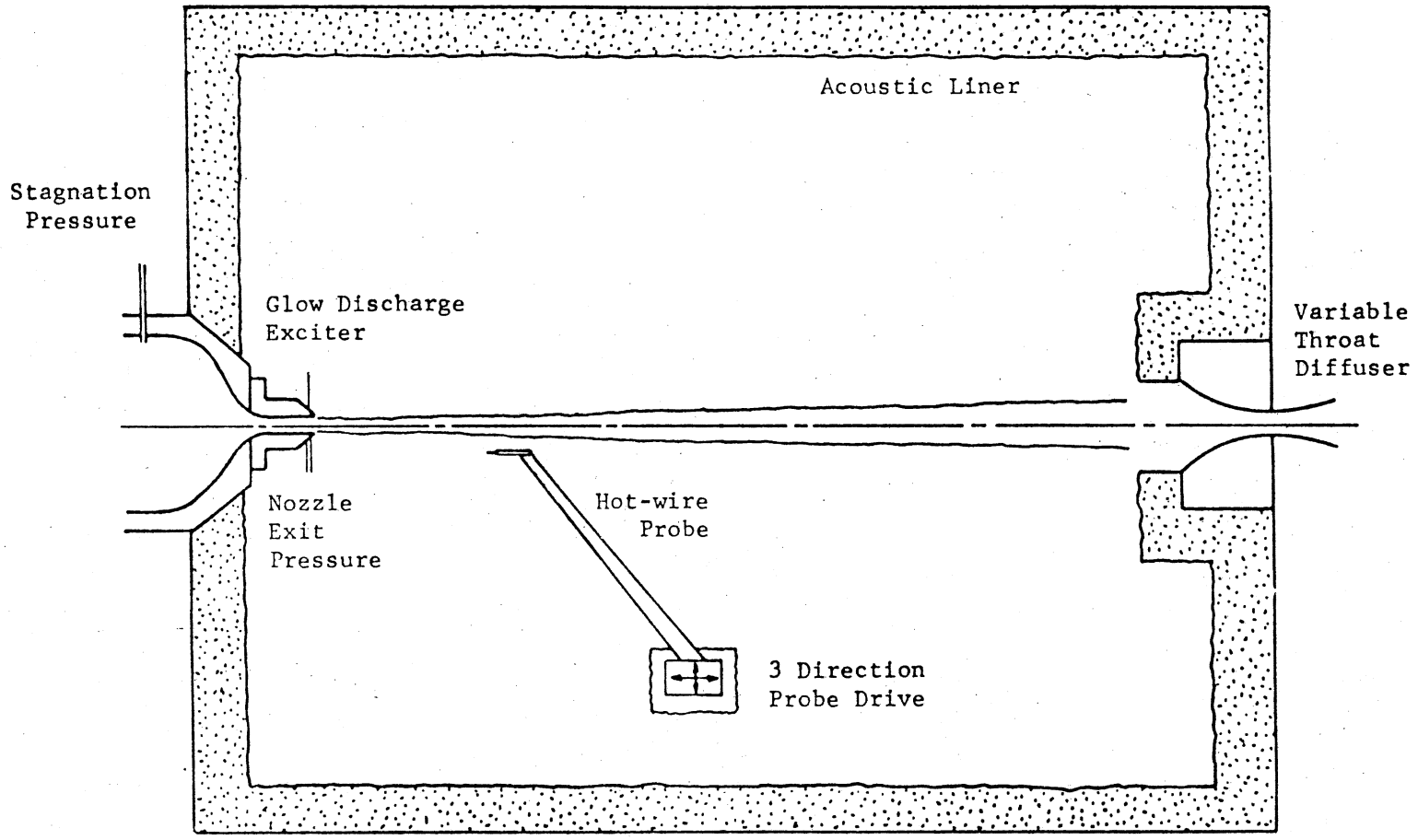

Figure 2. Schematic of Test Chamber

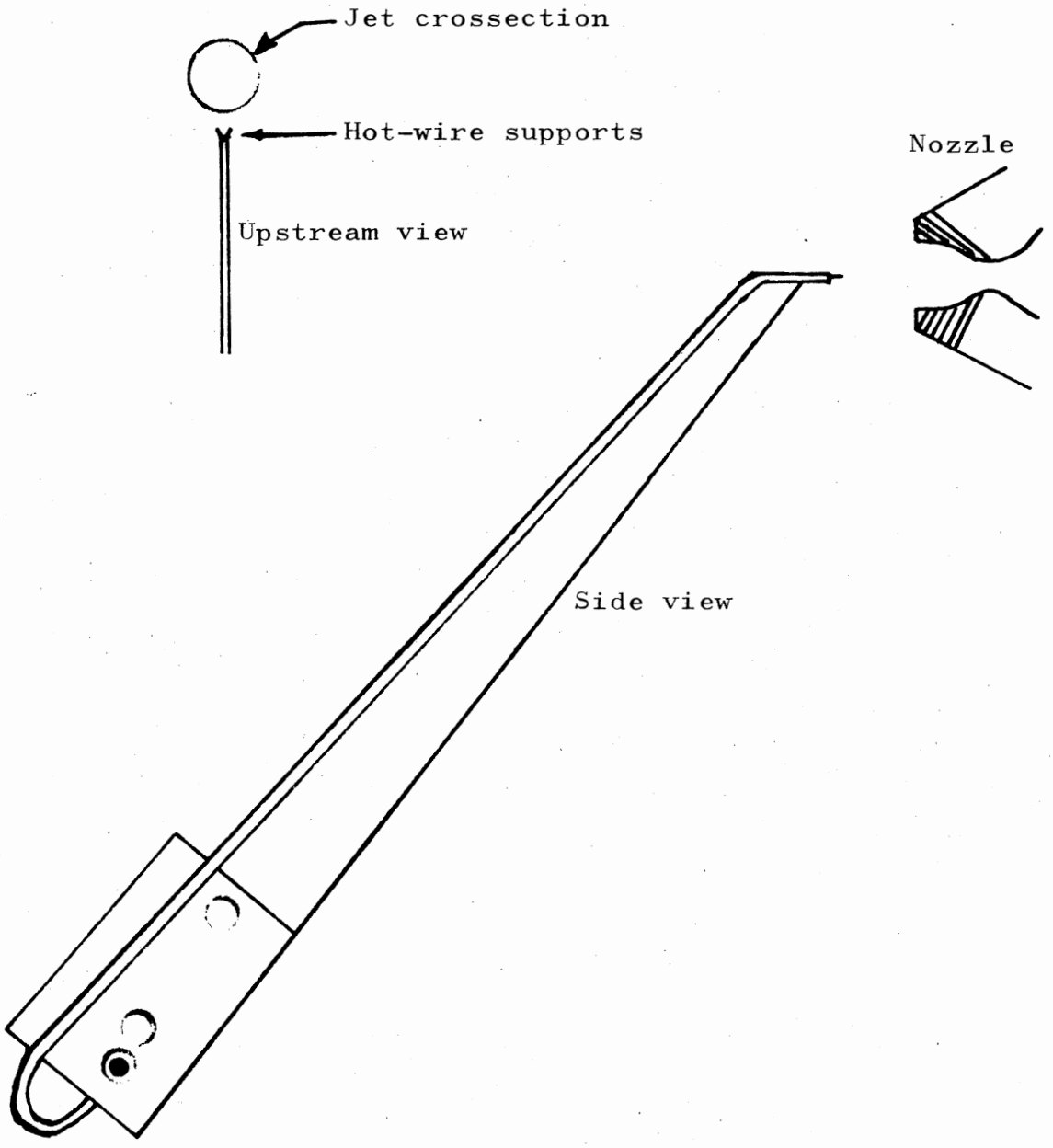

Figure 3. Hot-wire Probe, Full Scale

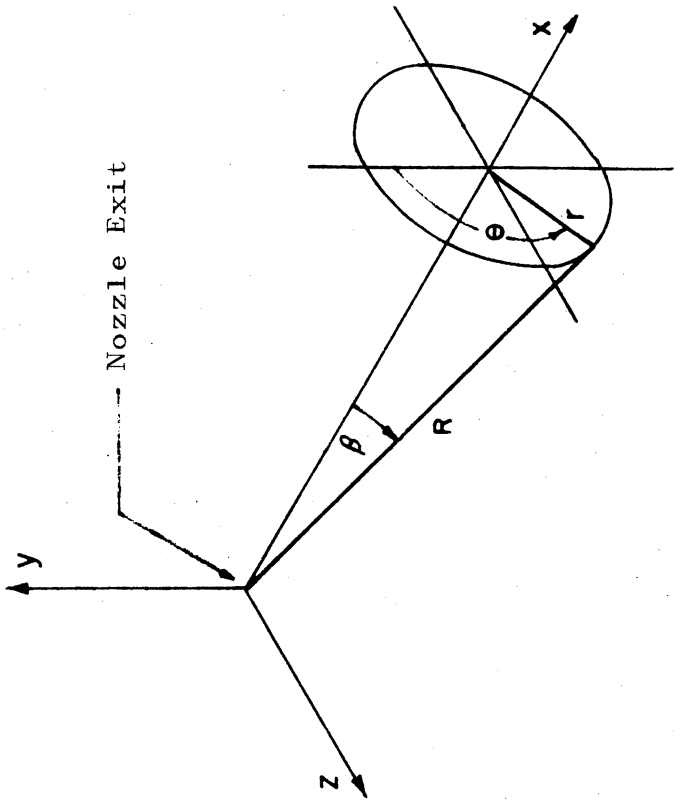

Figure 4. Coordinate Systems Diagram

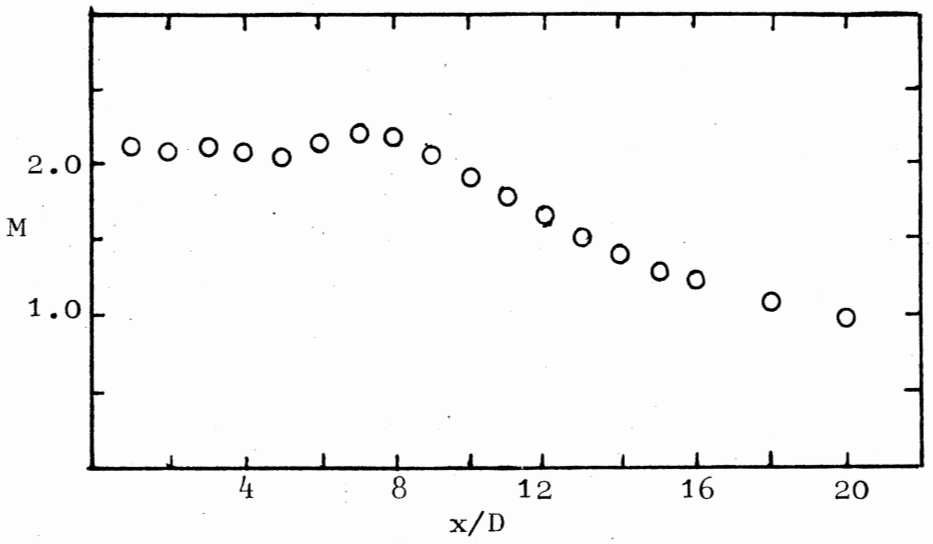

Figure 5. Mach Number on Jet Centerline

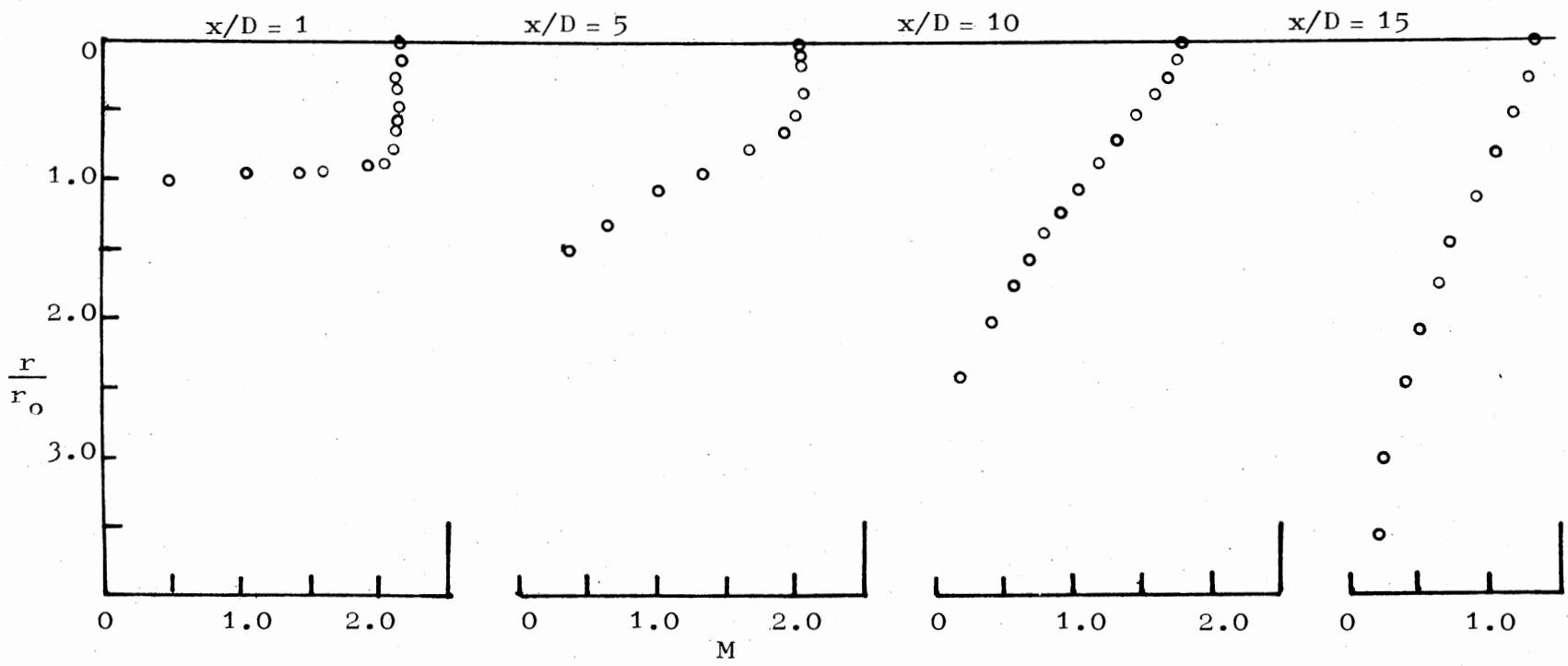

Figure 6. Radial Mach Number Profiles

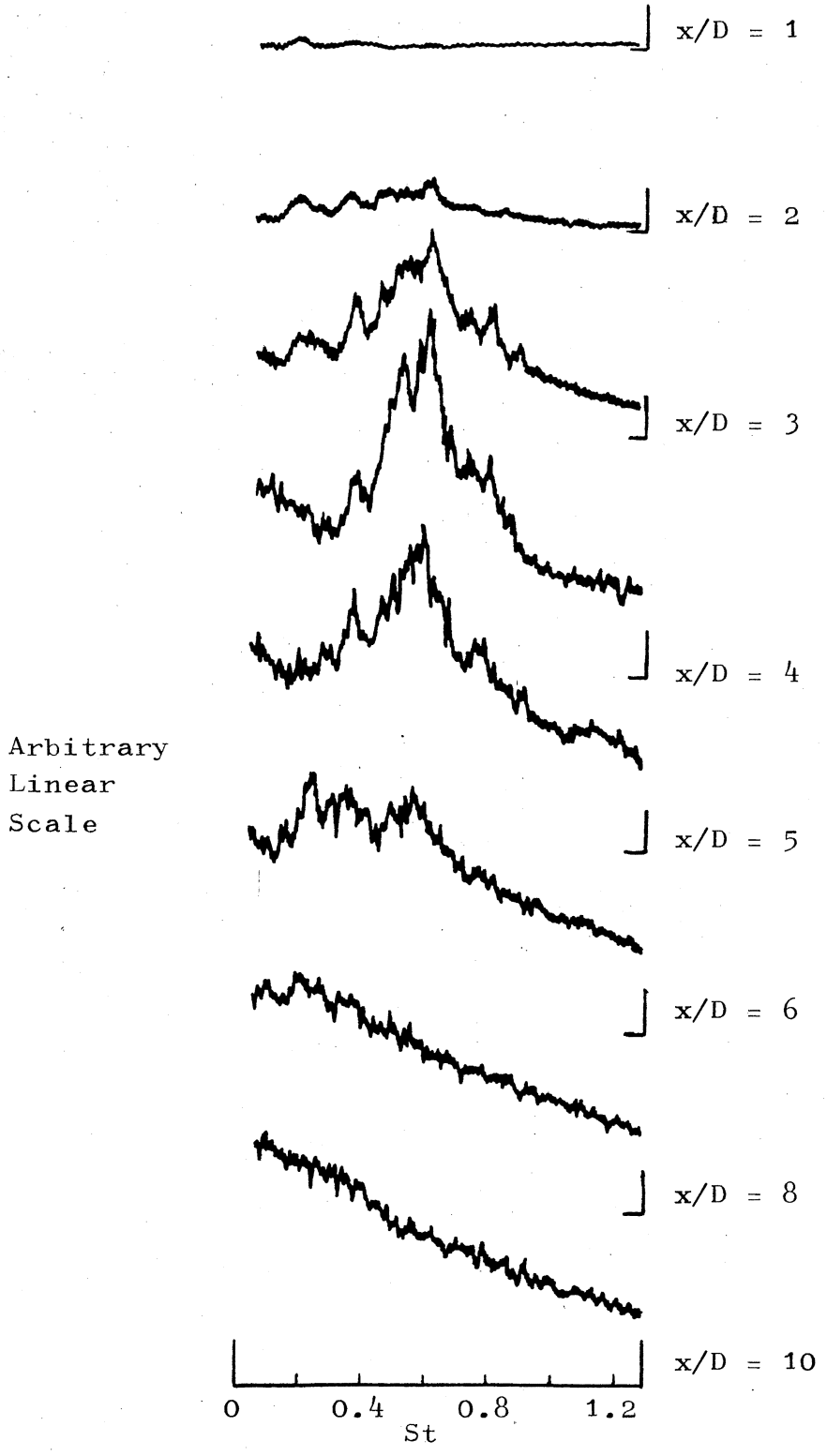

Figure 7. Hot-wire Spectra in the Jet Shear Layer

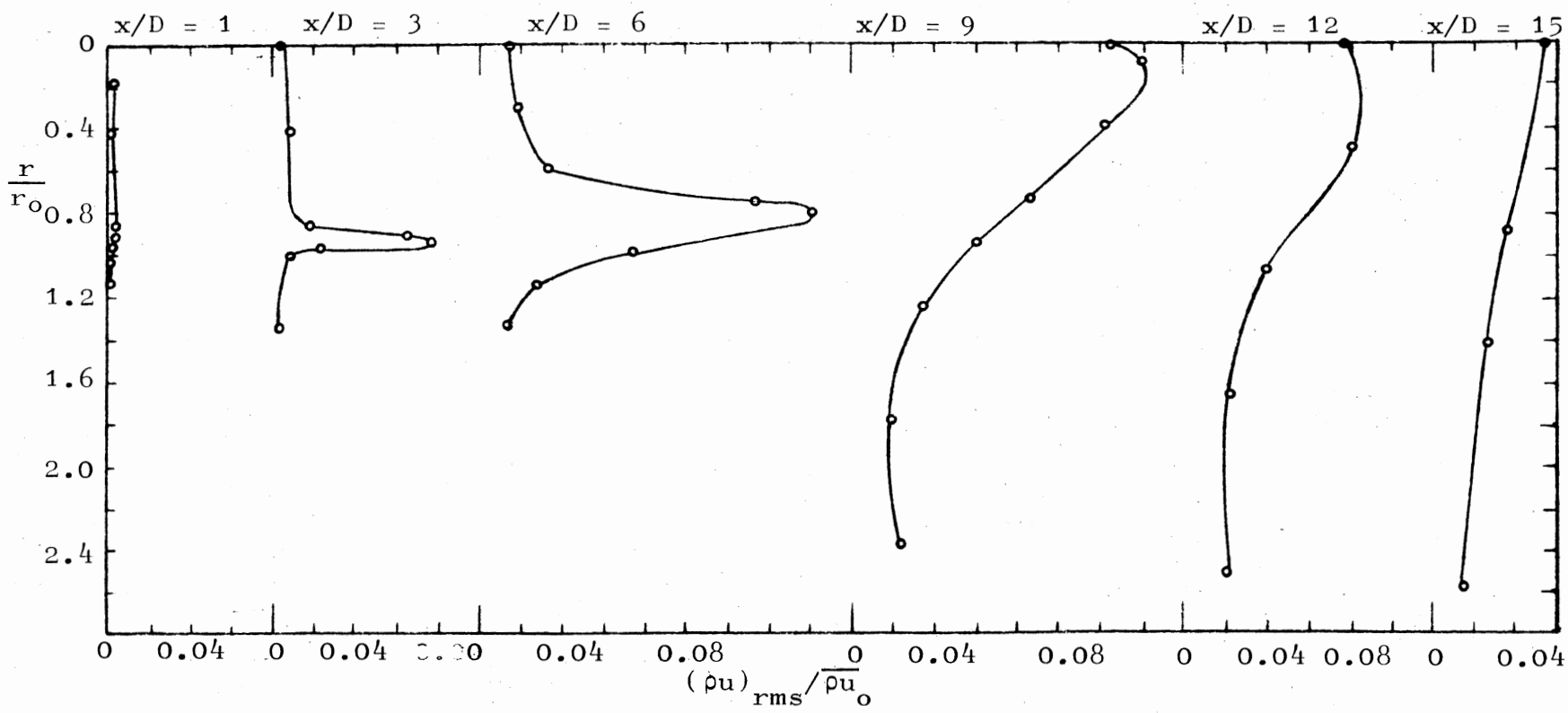

Figure 8. Radial Profiles of Mass-Velocity Fluctuation Amplitude

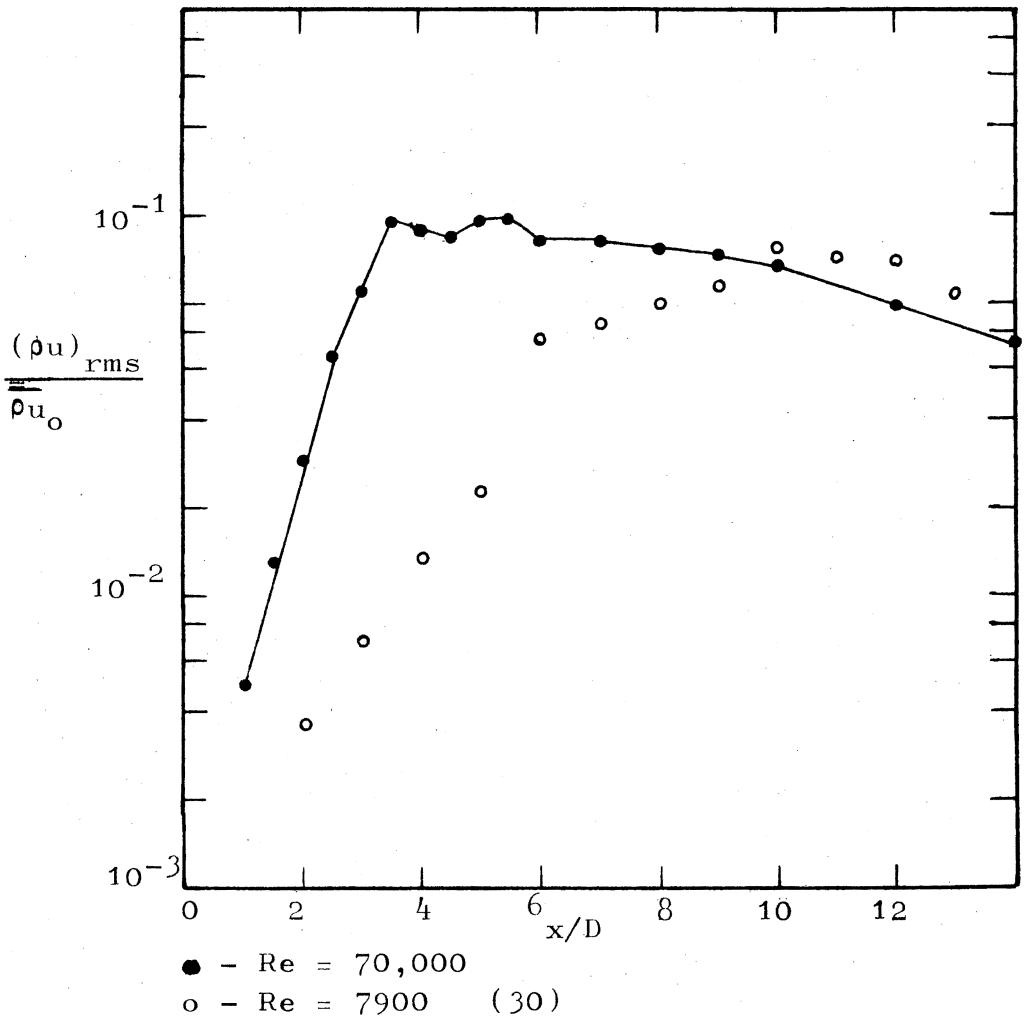

Figure 9. Total Mass-Velocity Fluctuation Amplitude in the Jet Shear Layer

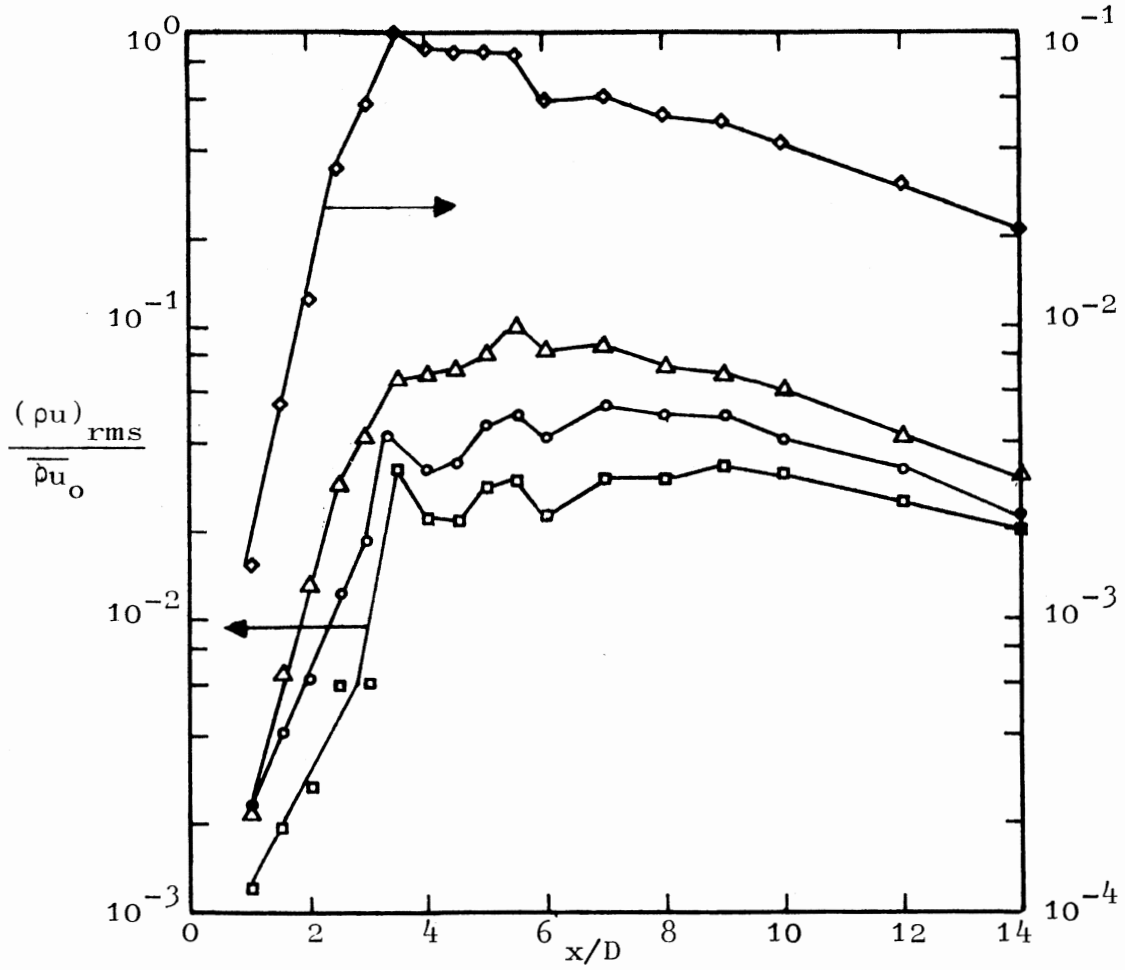

Figure 10. Band-Passed Mass-Velocity Fluctuation Amplitude in the Jet Shear Layer

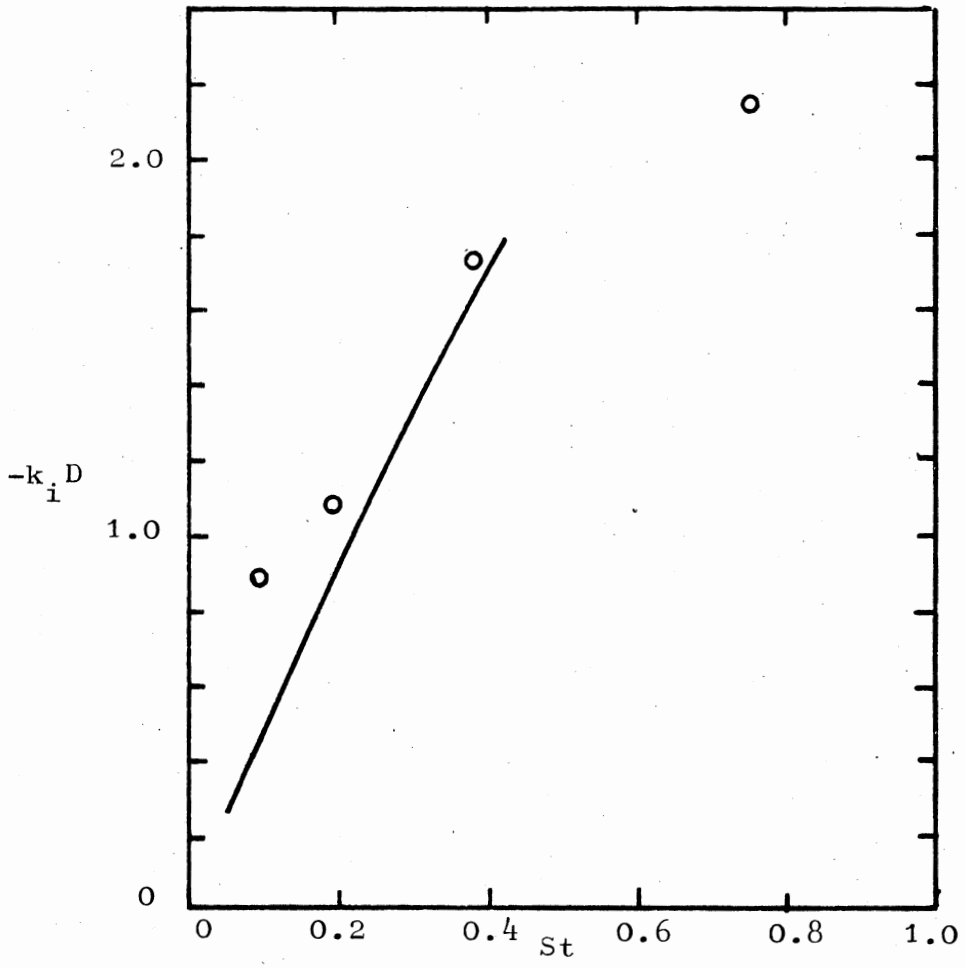

o - Re = 70,000 Experiments
(—) - Tam (21) Prediction

Figure 11. Initial Mass-Velocity Fluctuation Growth Rates

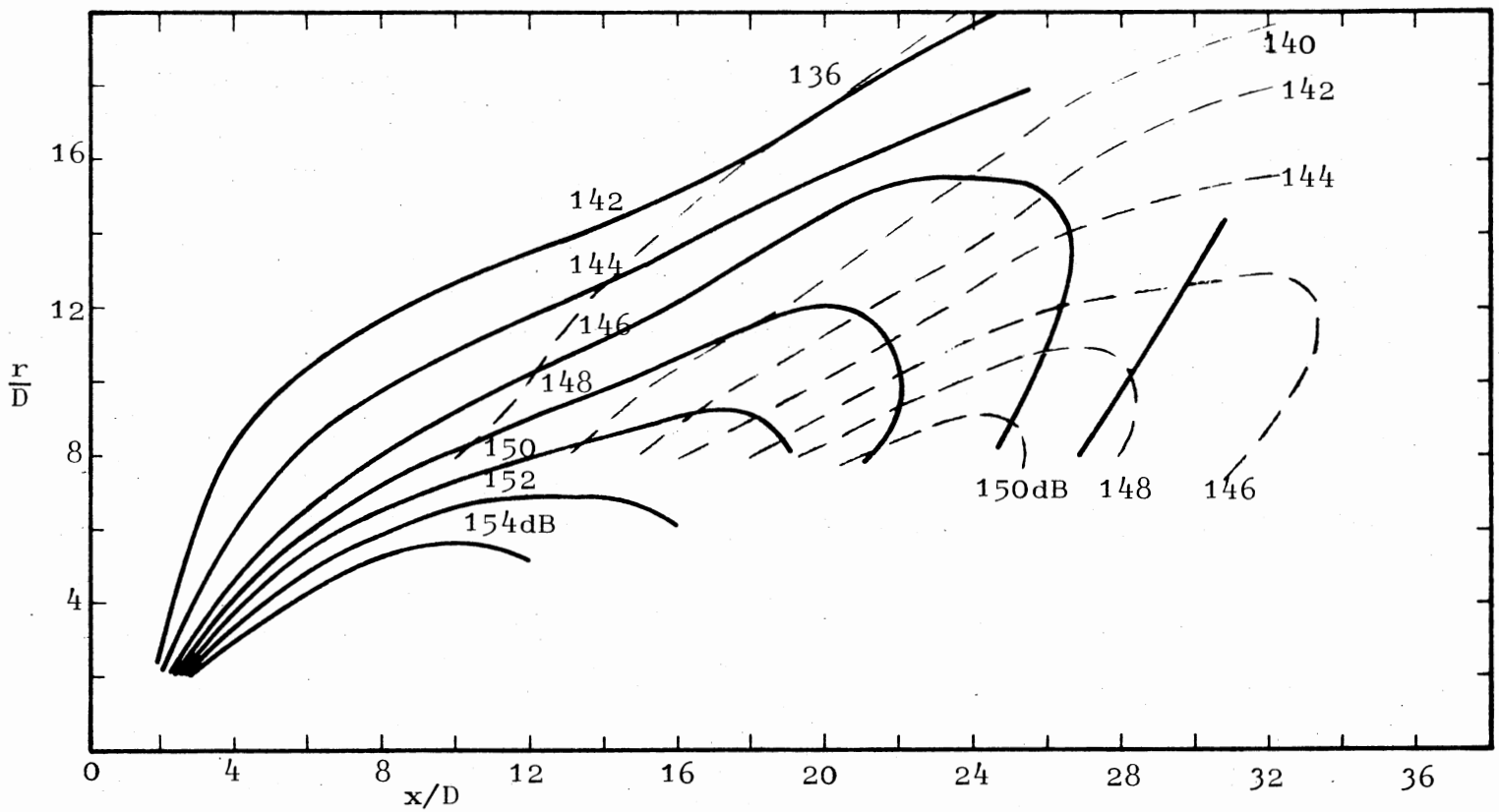

(---) Re = 7900 (30.); (——) Re = 70,000

Figure 12. Total Sound Pressure Level Contours

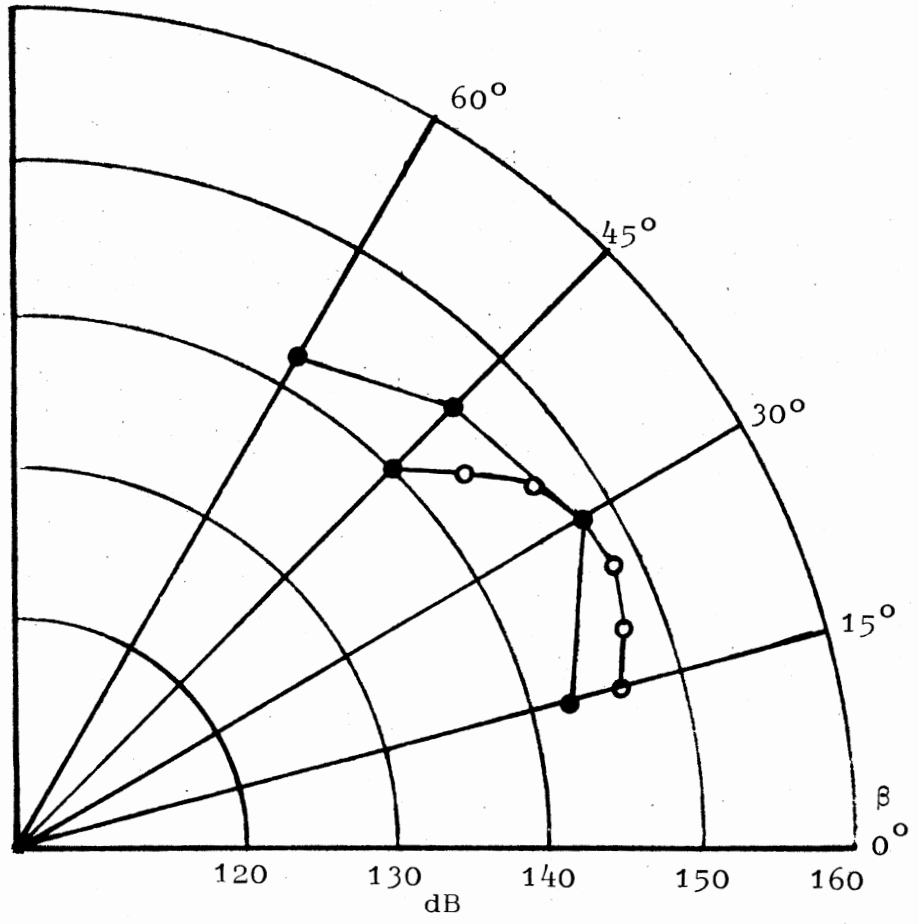

o - Re = 70,000
● - Re = 1.3×10^6 (40)
R/D = 24

Figure 13. Directivity Plot of Total Sound Pressure Level

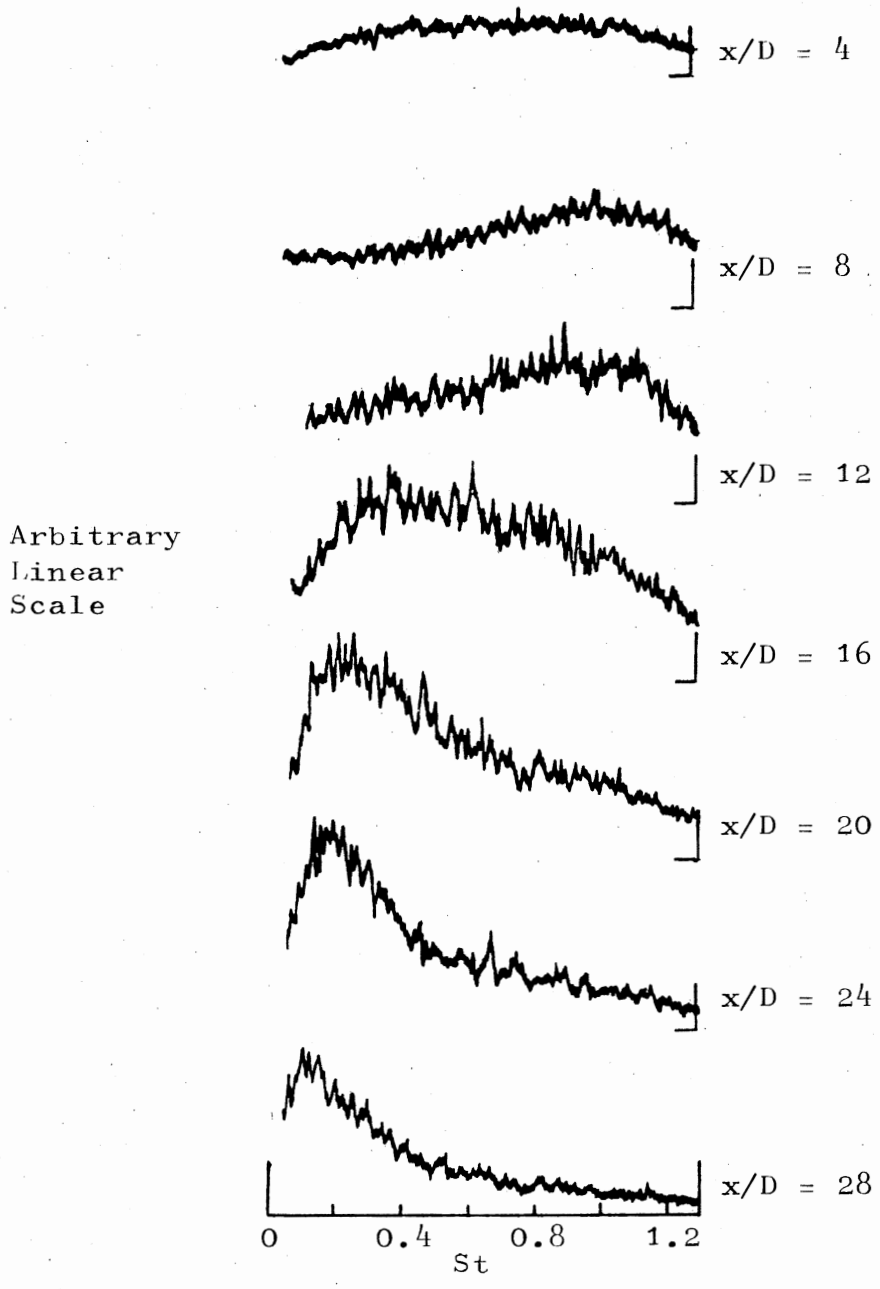

Figure 14. Acoustic Spectra, r/D = 8

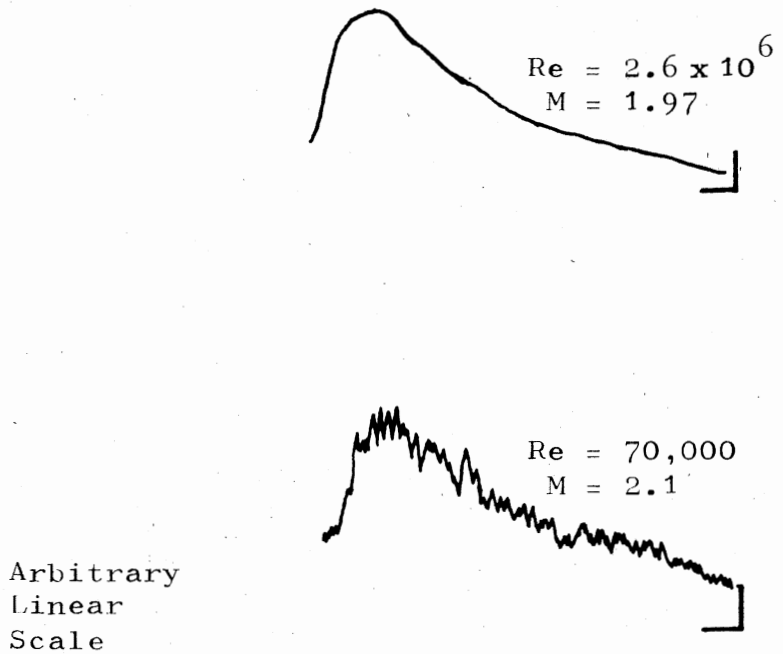

Re = 2.6×10^6 (19)
Re = 7900 (30)

Figure 15. Acoustic Spectra From Major Noise Production Region

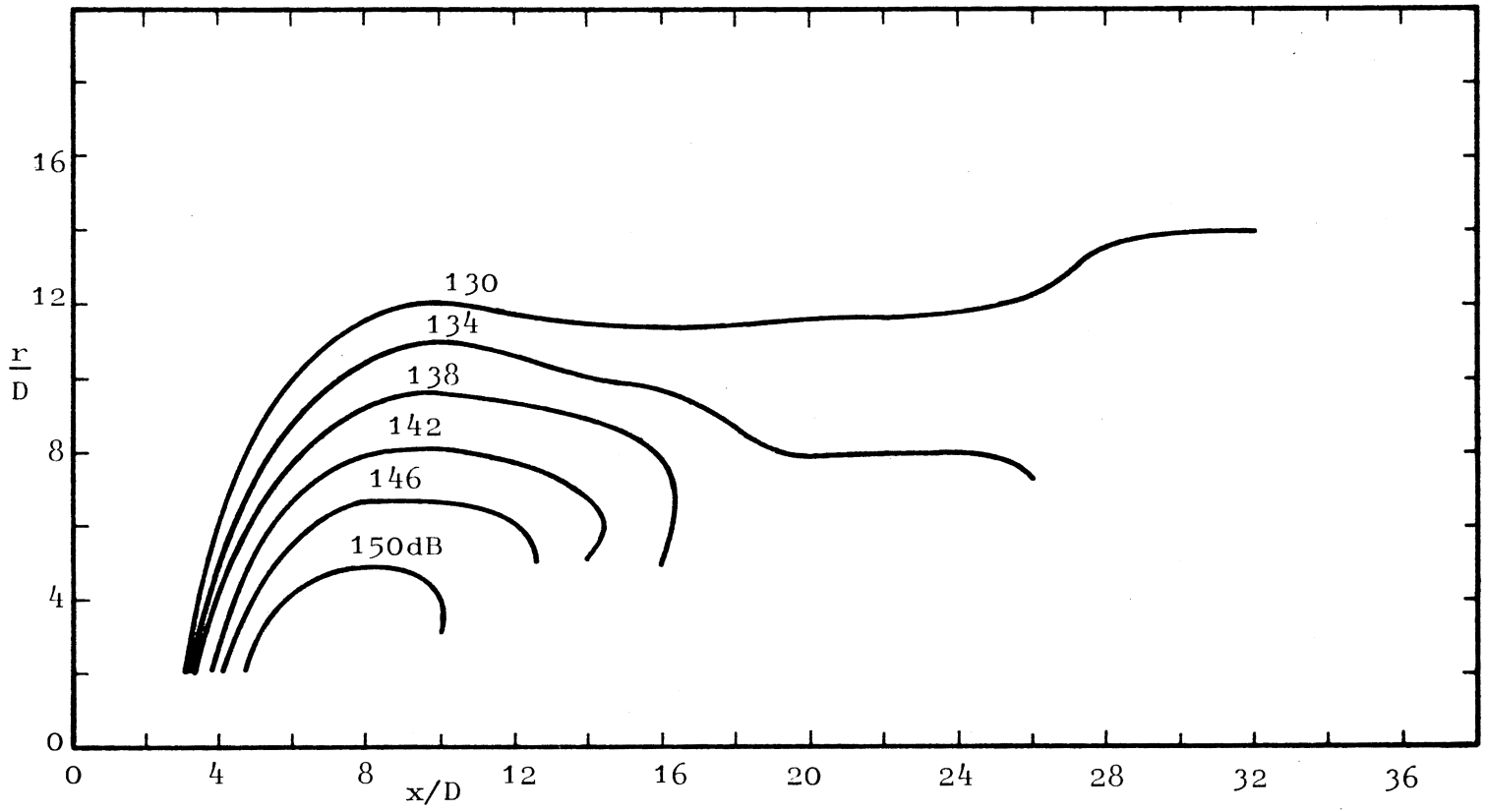

(a) St = 0.076 - .012

Figure 16. Band-Passed Sound Pressure Level Contours

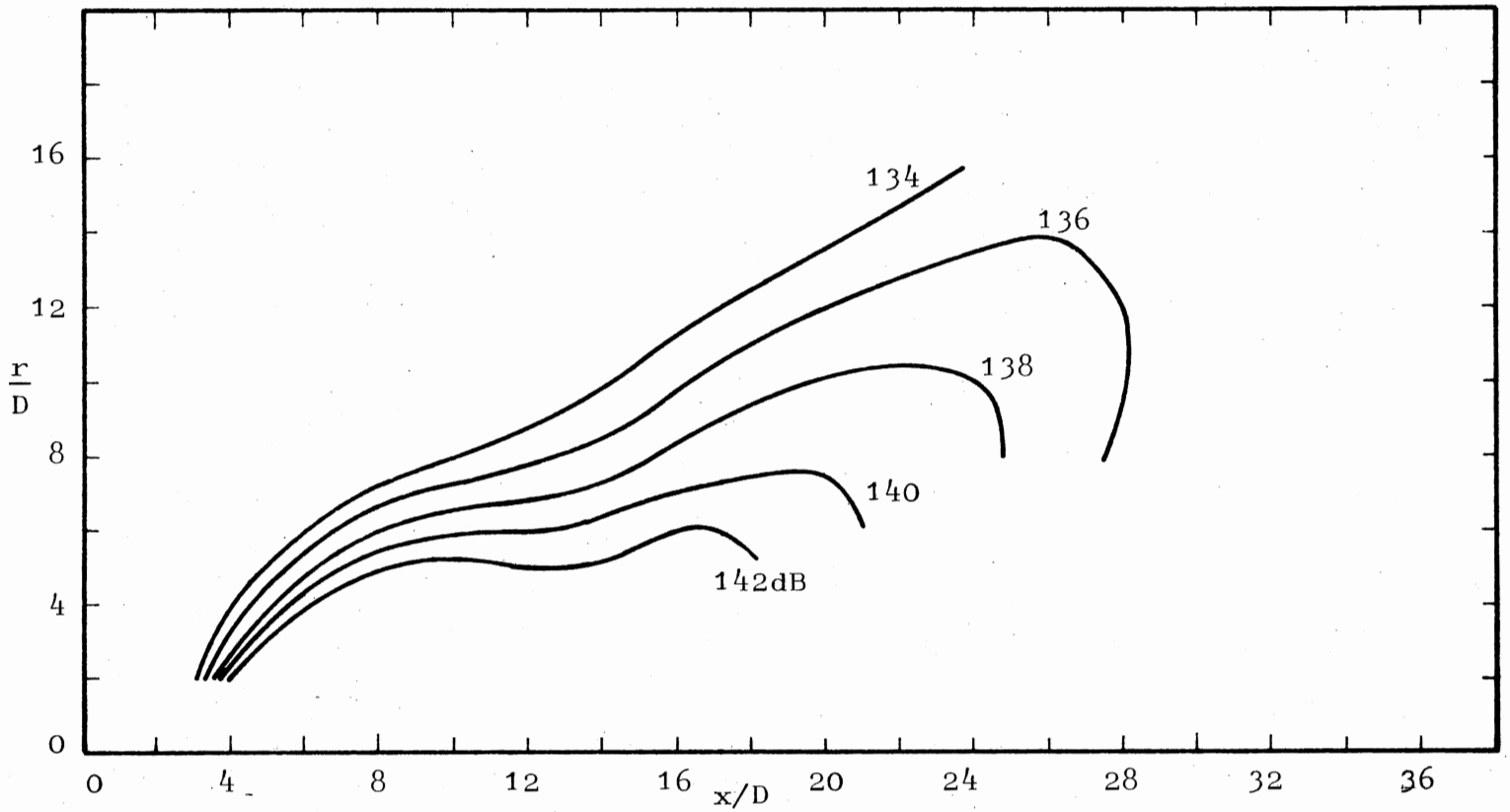

(b) St = 0.151 - 0.226

Figure 16. (Continued)

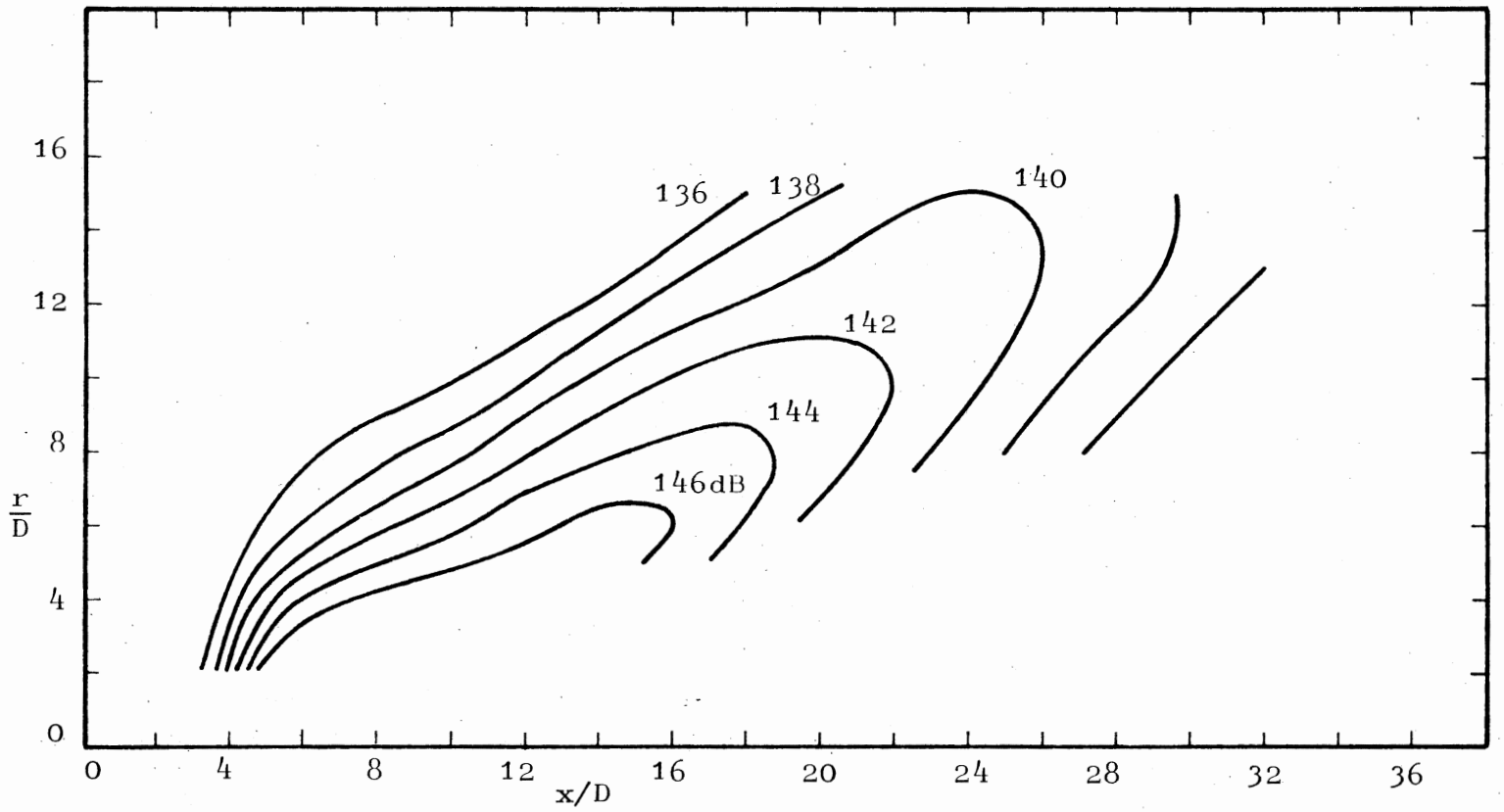

(c) St = 0.30 - 0.45

Figure 16. (Continued)

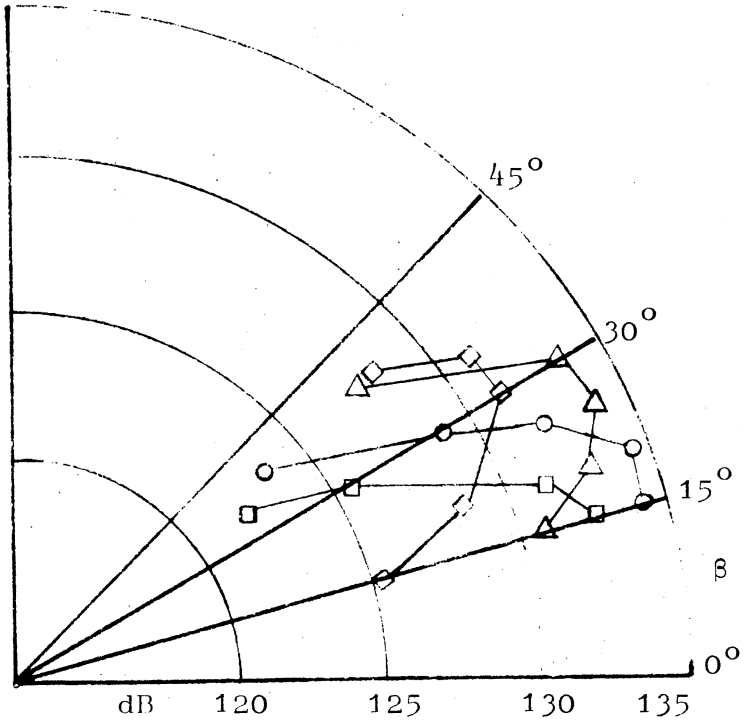

Figure 17. Band-Passed Sound Pressure Level Directivity Plots

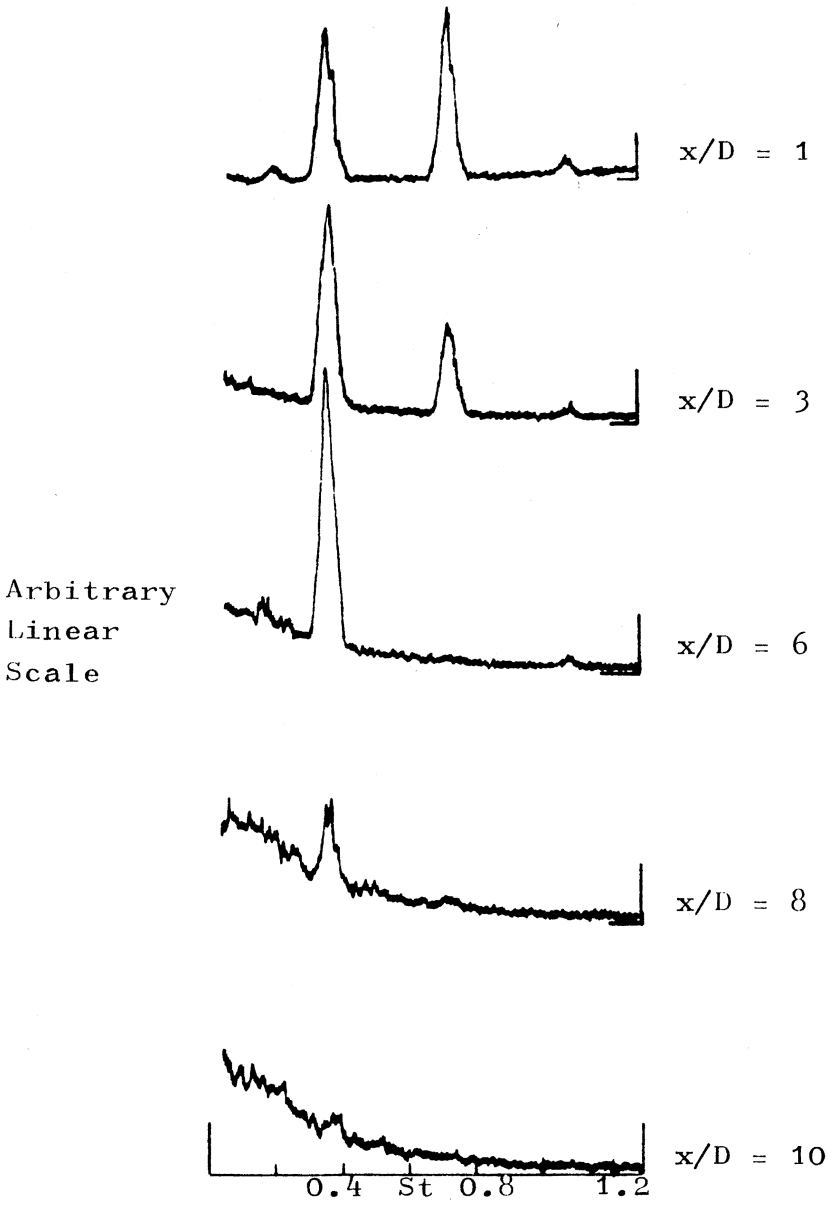

Figure 18. Hot-Wire Spectra in Jet Shear Layer; Jet Excited at St = 0.38

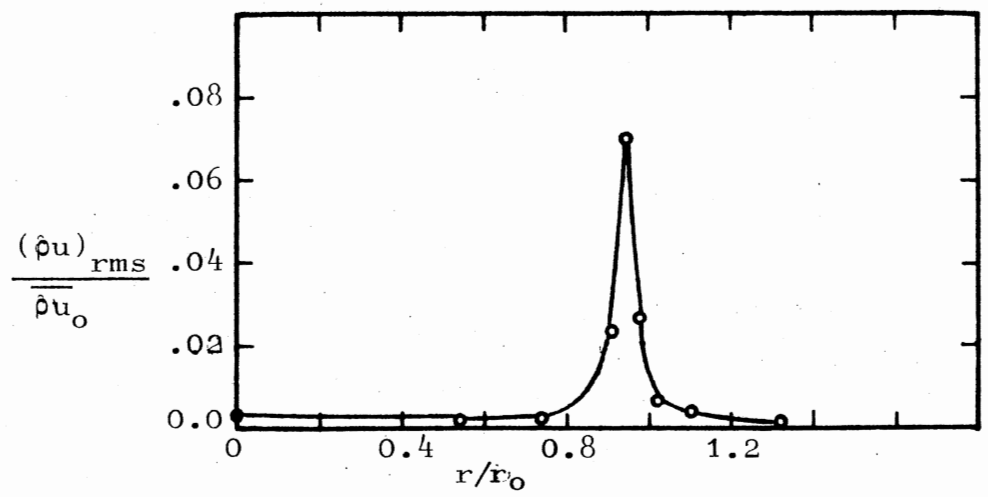

Figure 19. Radial Profile of Mass-Velocity Fluctuation Amplitude x/D = 1; Jet Excited at St = 0.19

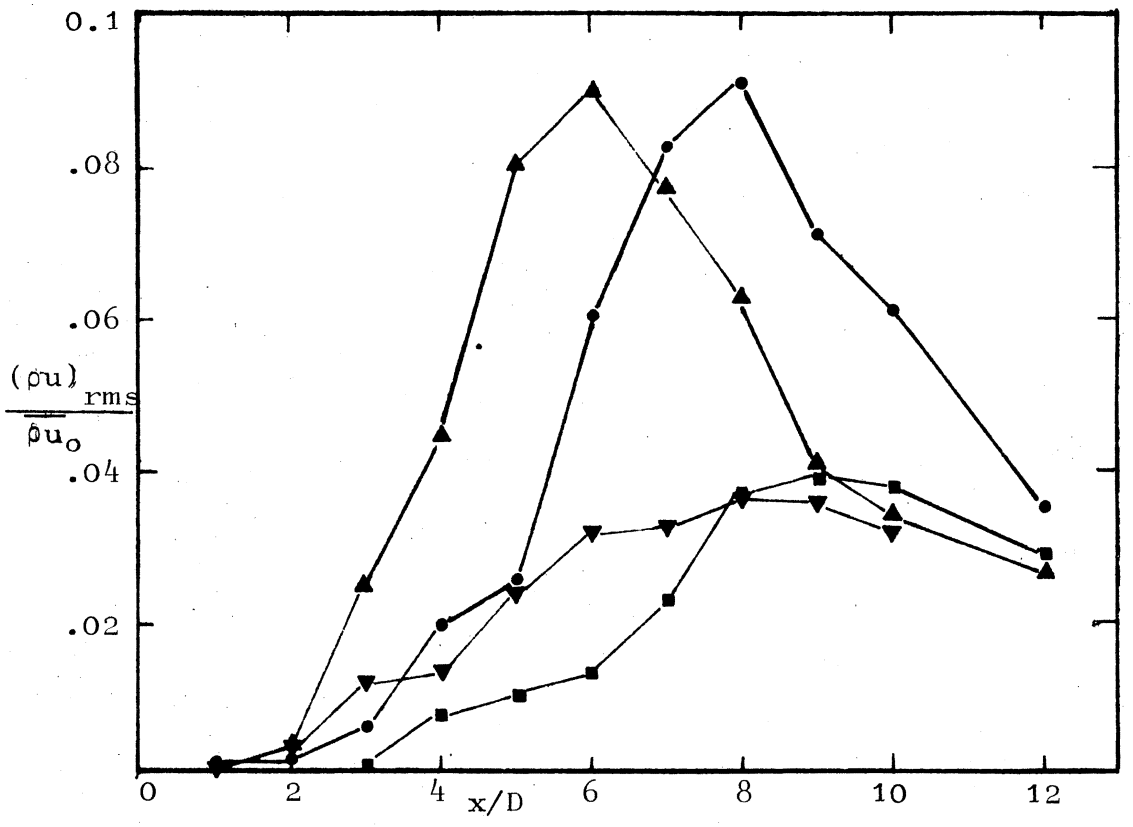

Figure 20. Band-Passed Mass-Velocity Fluctuation Amplitude on Jet Centerline

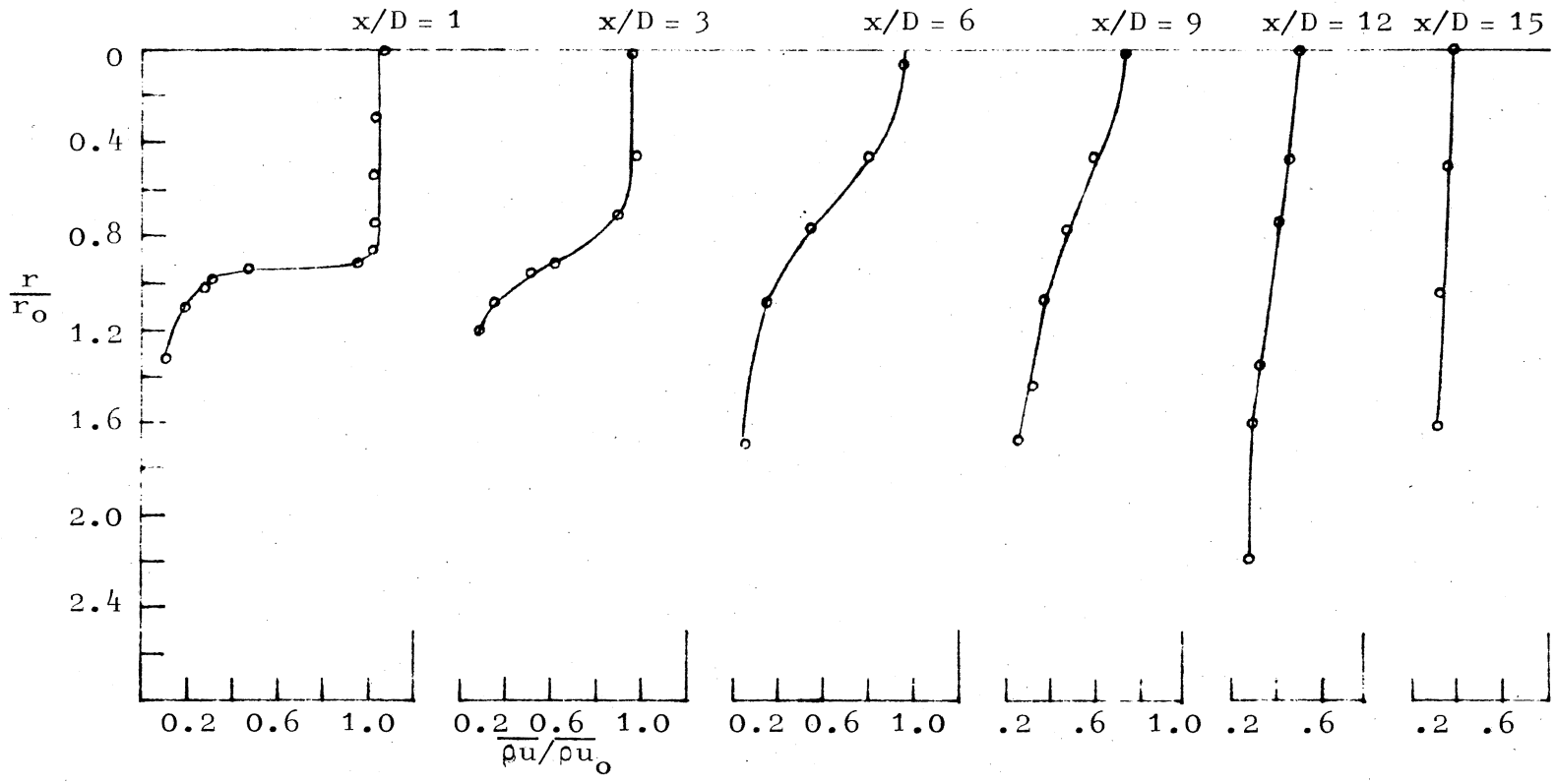

Figure 21. Radial Profiles of Mean Mass-Velocity Jet Excited at St = 0.19

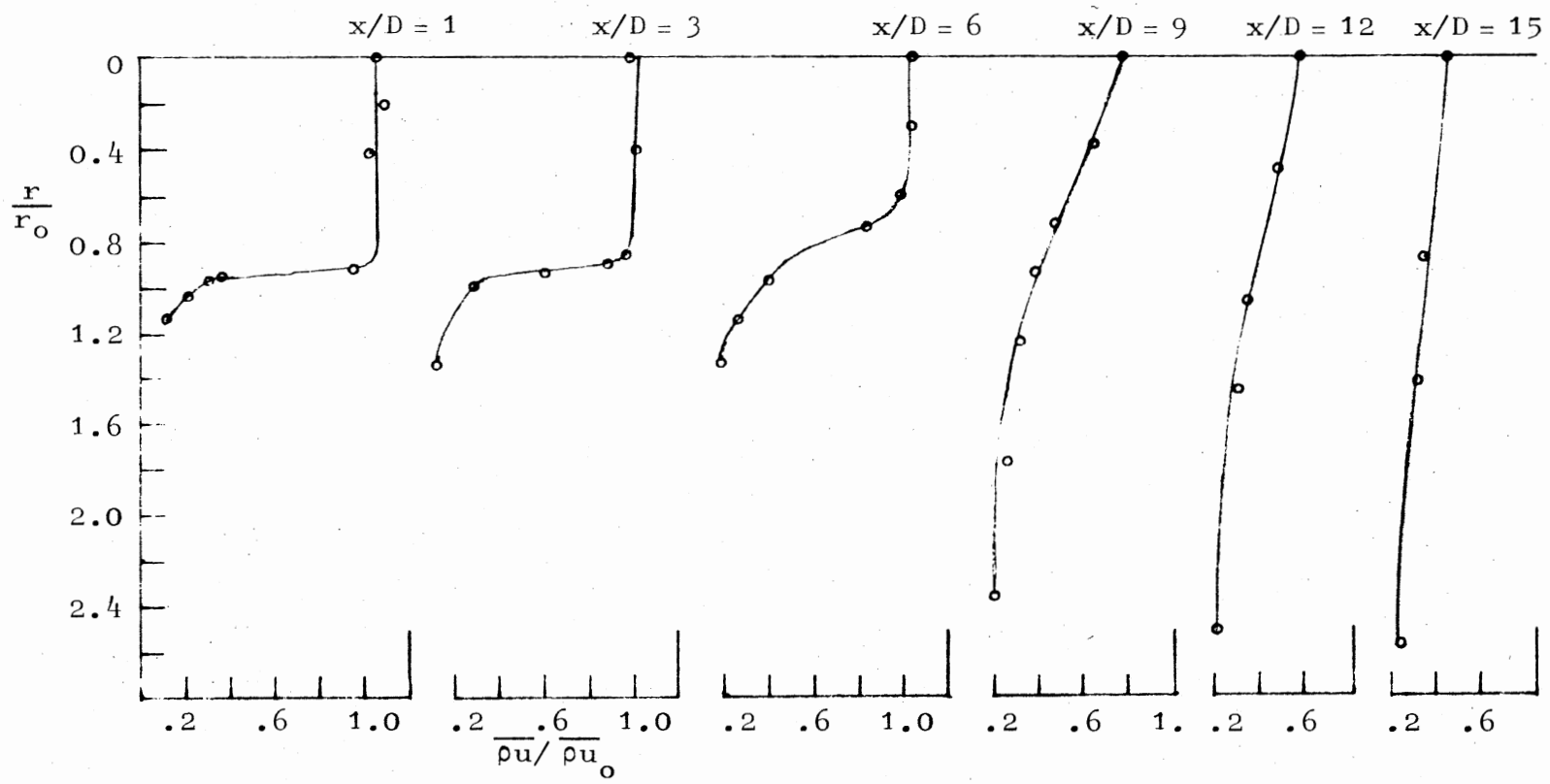

Figure 22. Radial Profiles of Mean Mass-Velocity; Jet Naturally Excited

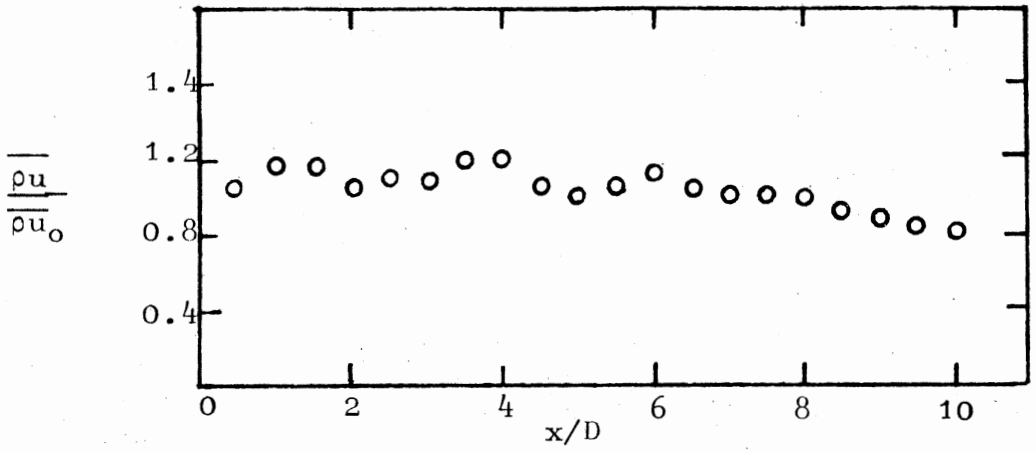

(a) Natural Jet

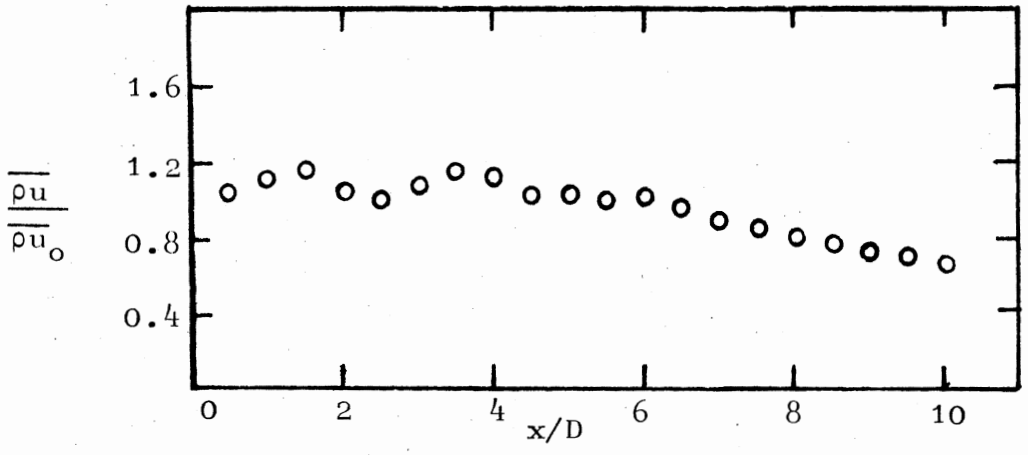

(b) Jet Excited at St = 0.19

Figure 23. Mean Mass-Velocity on Jet Centerline

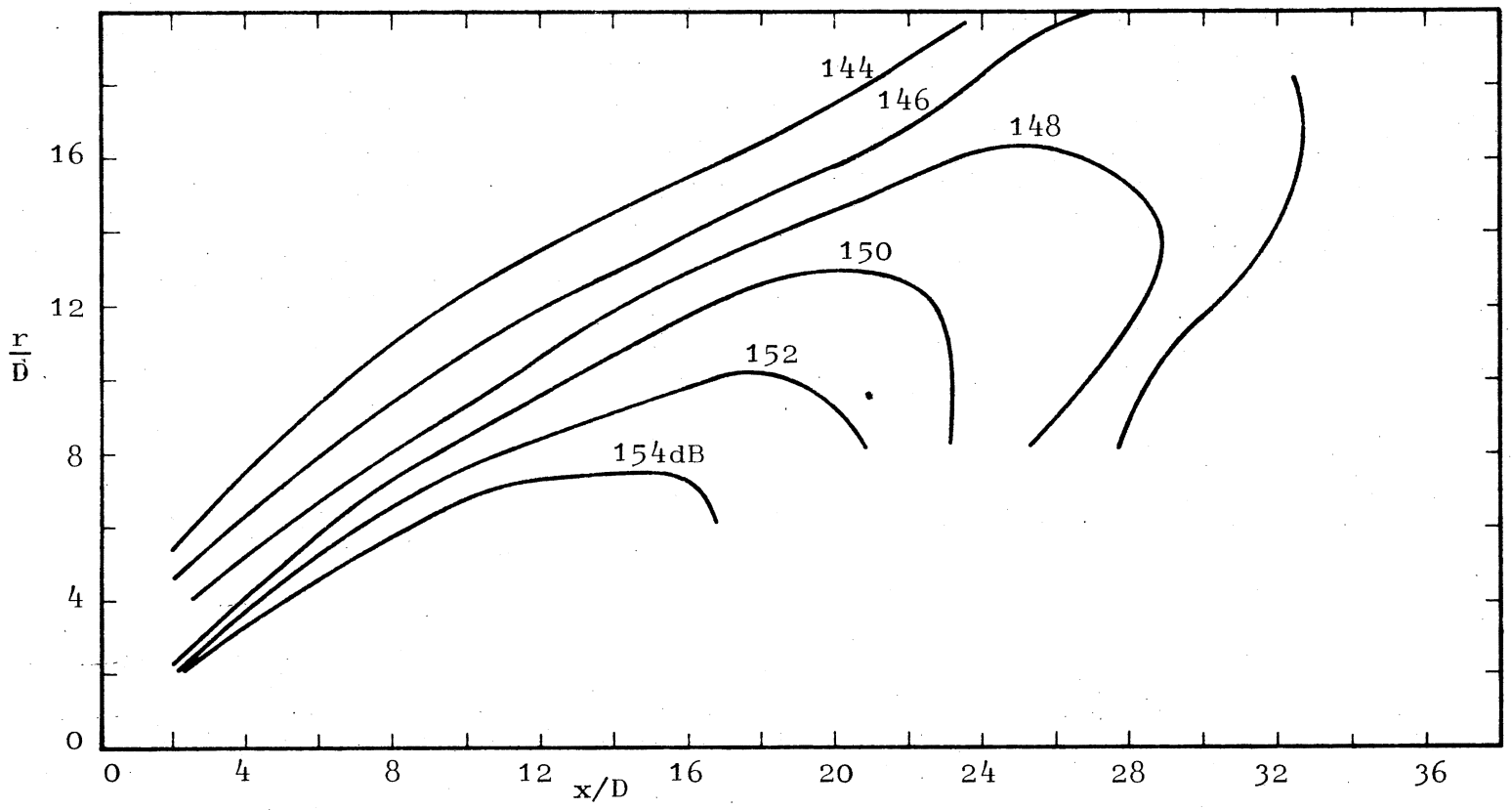

Figure 24. Total Sound Pressure Level Contours; Jet Excited at St = 0.19

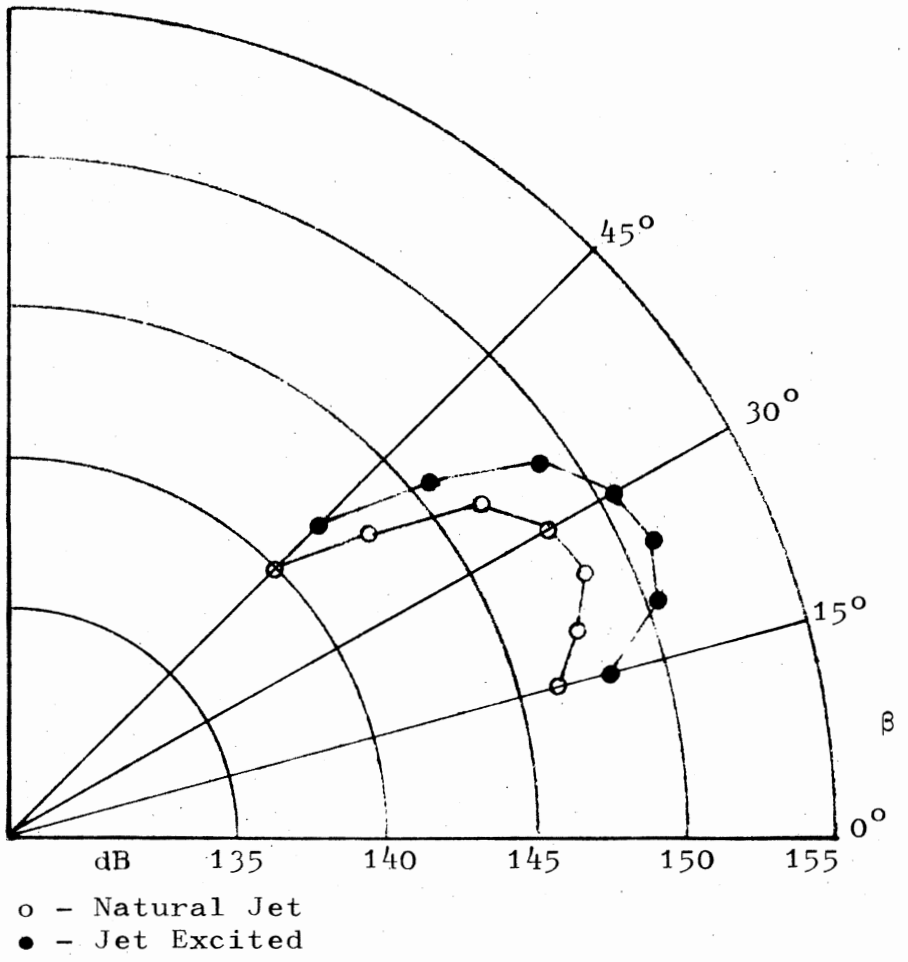

Figure 25. Total Sound Pressure Level Directivity Plot; Jet Excited

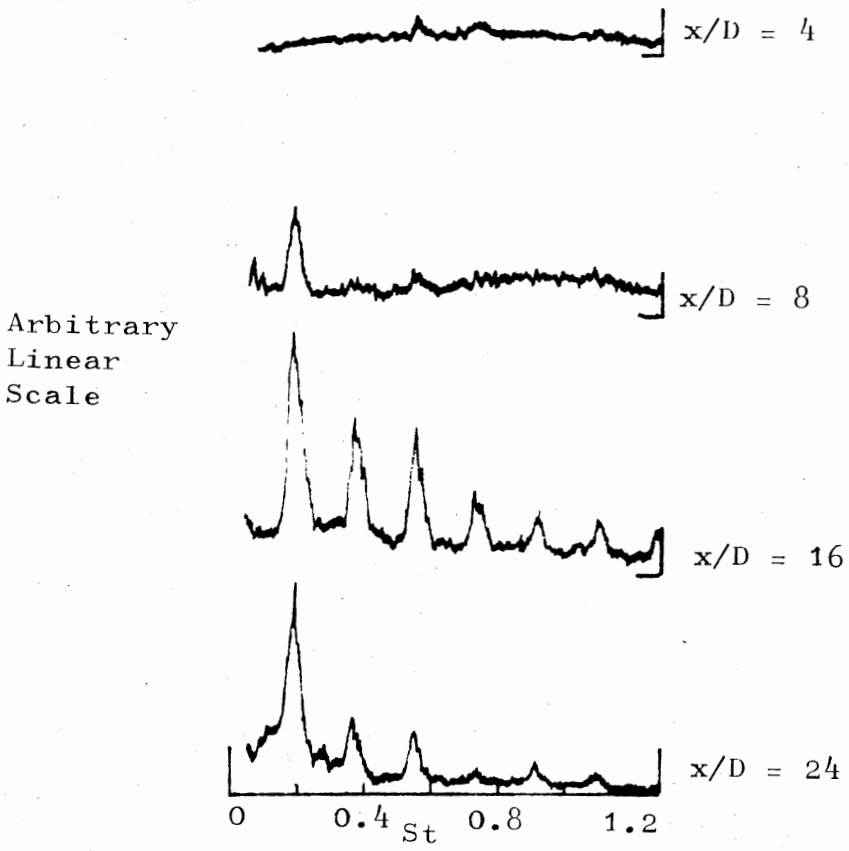

Figure 26. Acoustic Spectra, r/D = 8; Jet Excited at St = 0.19

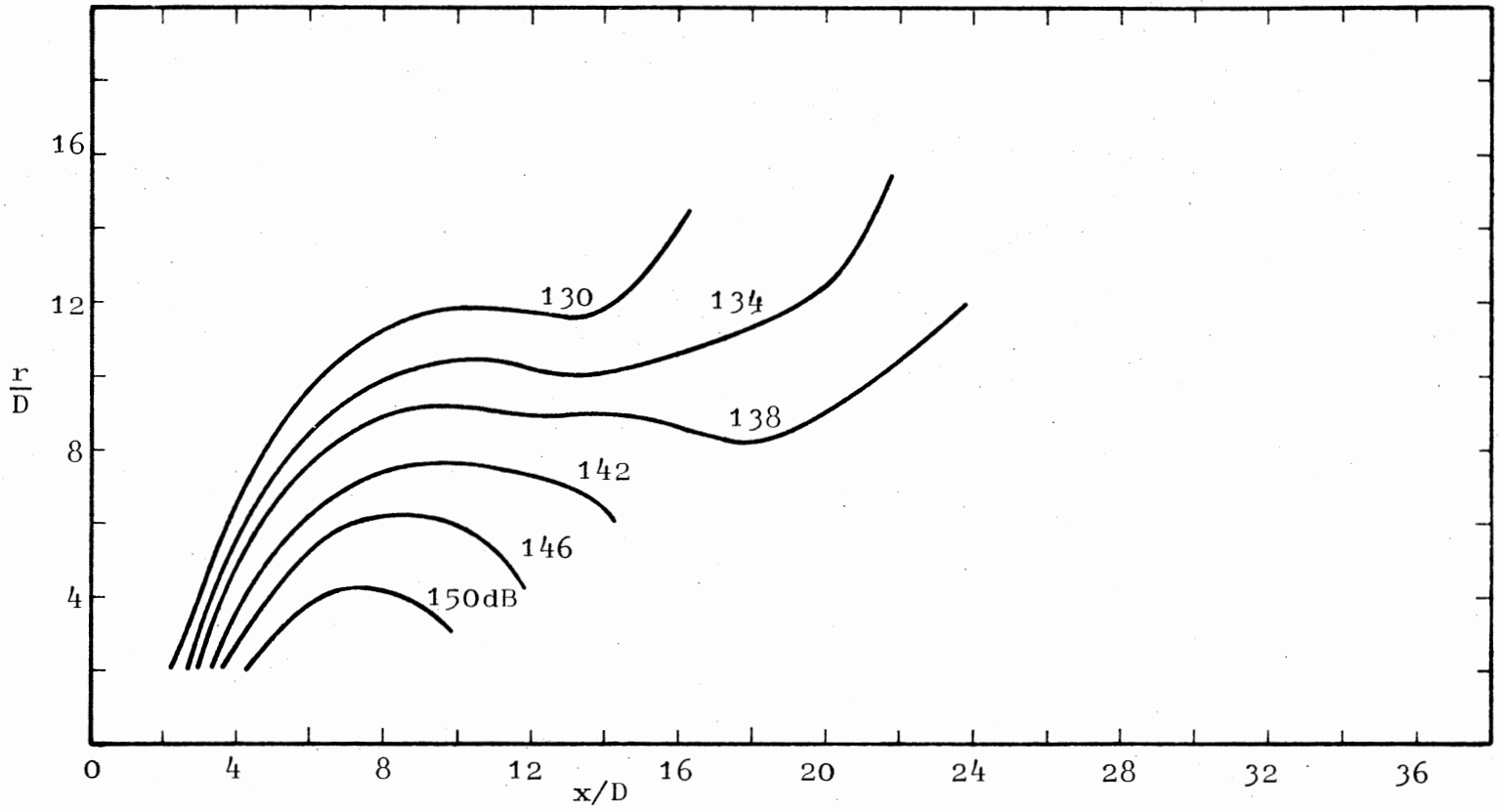

(a) St = 0.075 - 0.113; Excited at St = 0.094

Figure 27. Band-Passed Sound Pressure Level Contours for Excited Jet

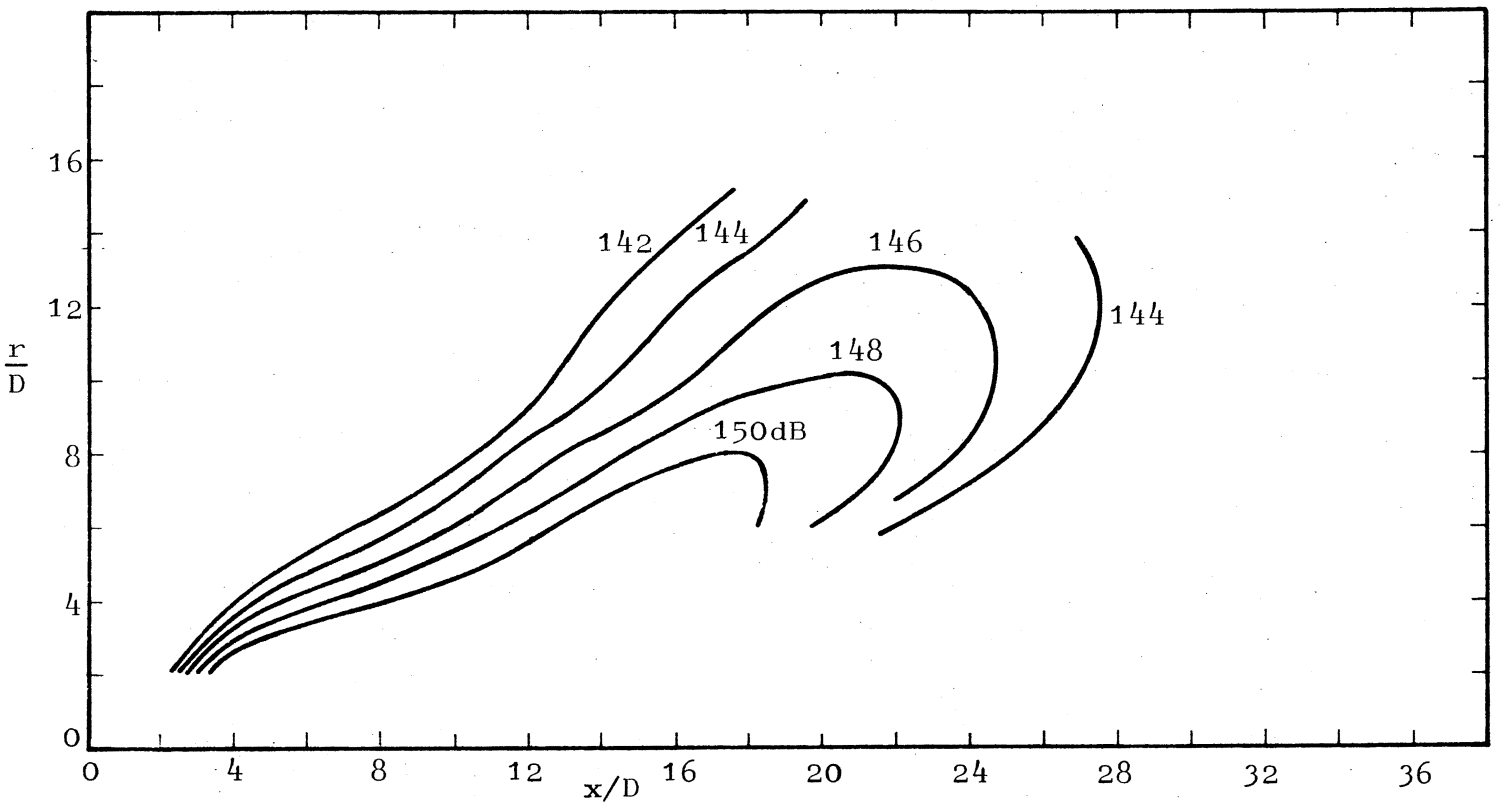

(b) St = 0.15 - 0.23; Excited at St = 0.19

Figure 27. (Continued)

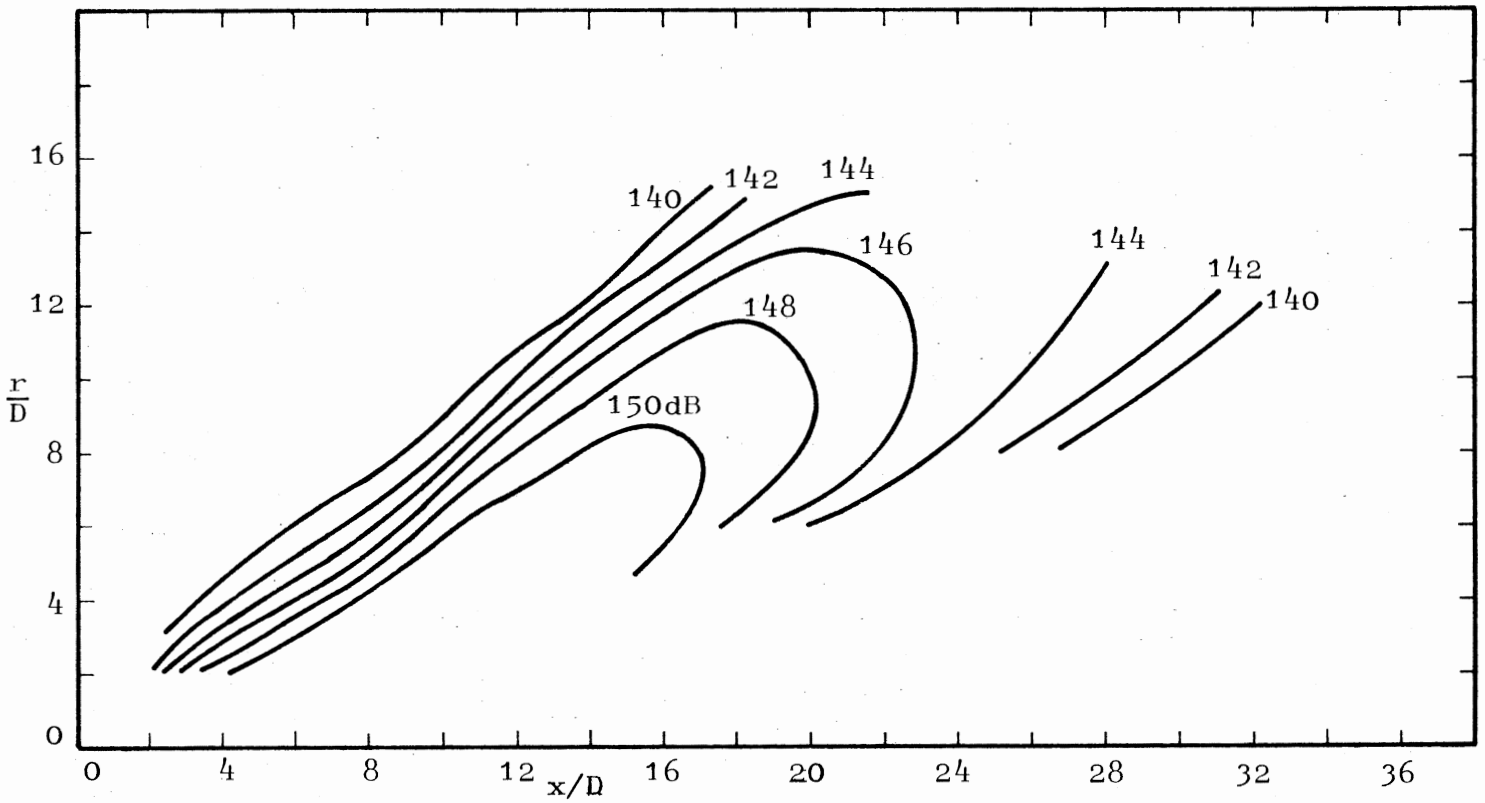

(c) St = 0.30 - 0.45; Excited at St = 0.38

Figure 27. (Continued)

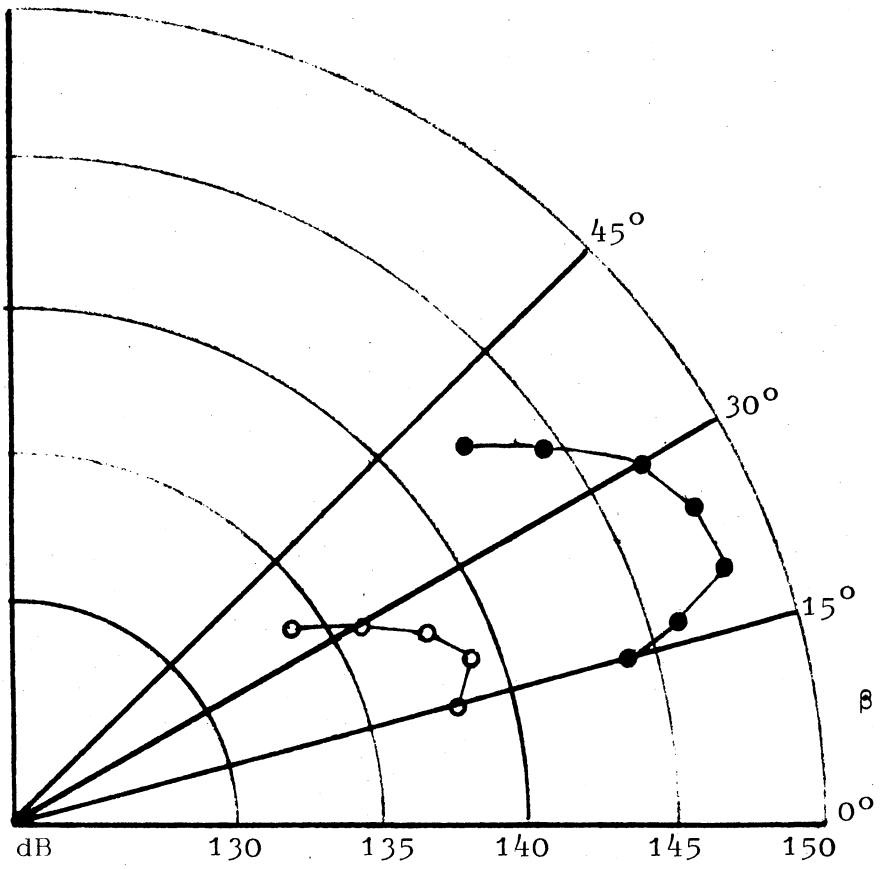

o - Natural Jet

● - Jet Excited St = 0.19

(a) St = 0.15 - 0.23

Figure 28. Band-Passed Sound Pressure Level Directivity Plots

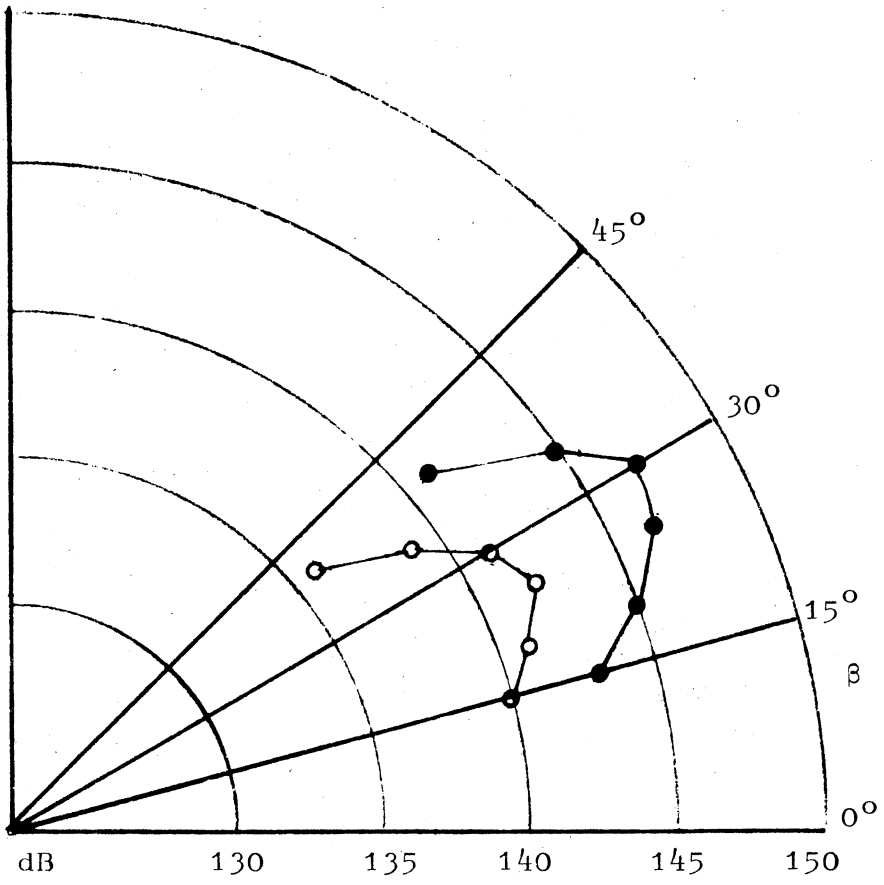

o - Natural Jet
● - Jet Excited St = 0.38

(b) St = 0.30 - 0.45

Figure 28. (Continued)

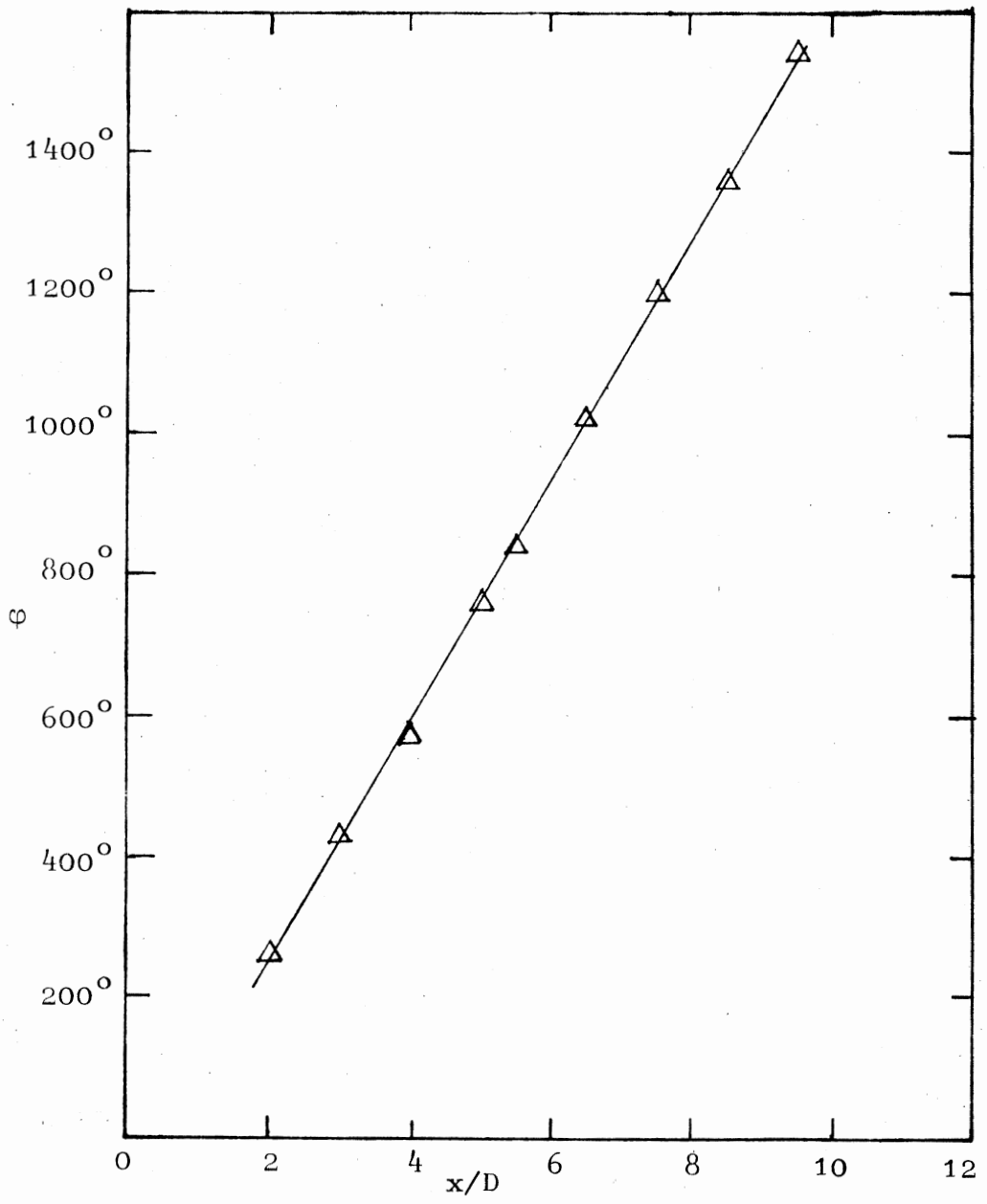

Figure 29. Flow Disturbance Phase Angle; Jet Excited at St = 0.38

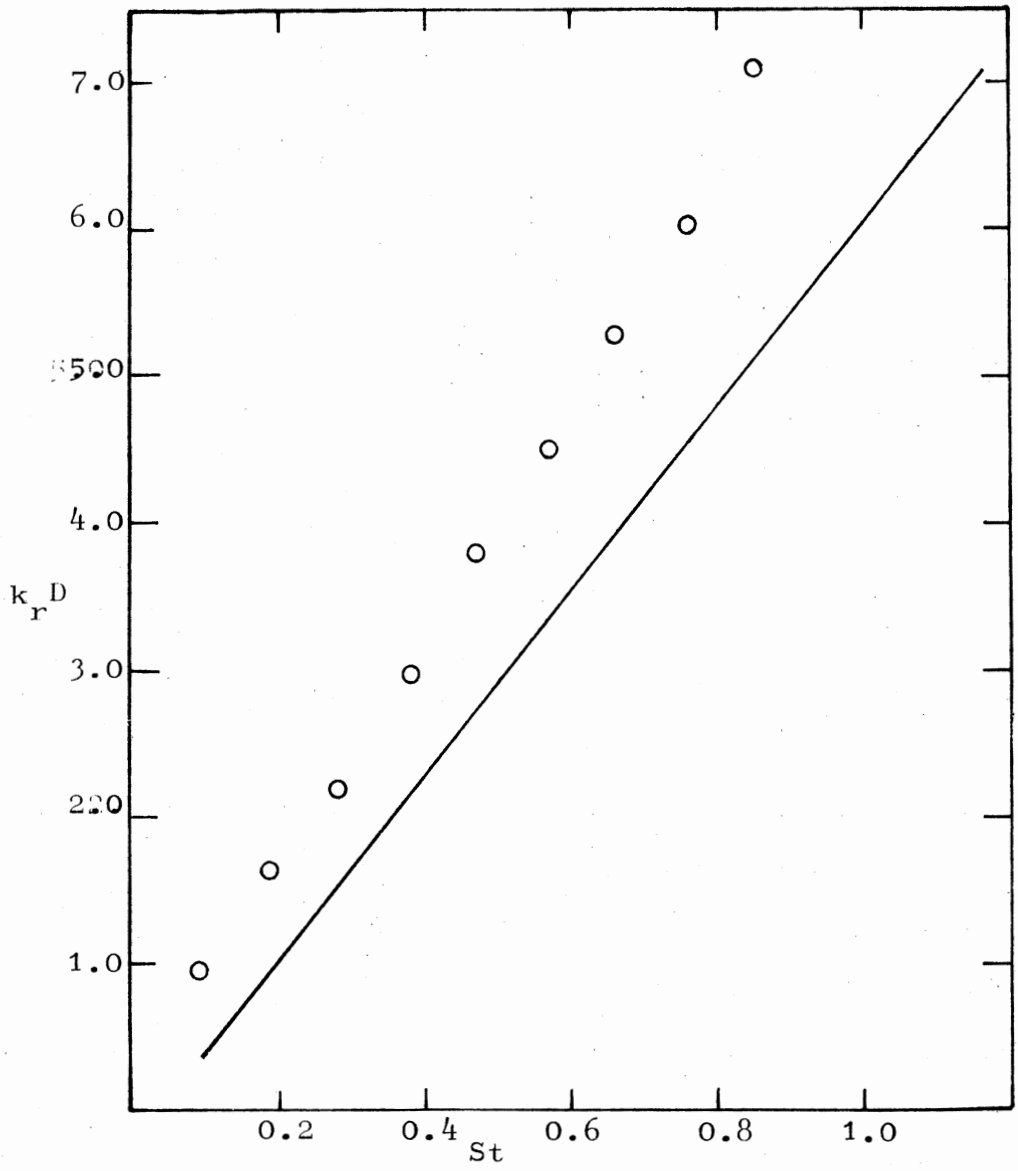

o - Present Study
(-) - Tam (21) Theoretical Prediction

Figure 30. Axial Wavenumbers of Excited Disturbances

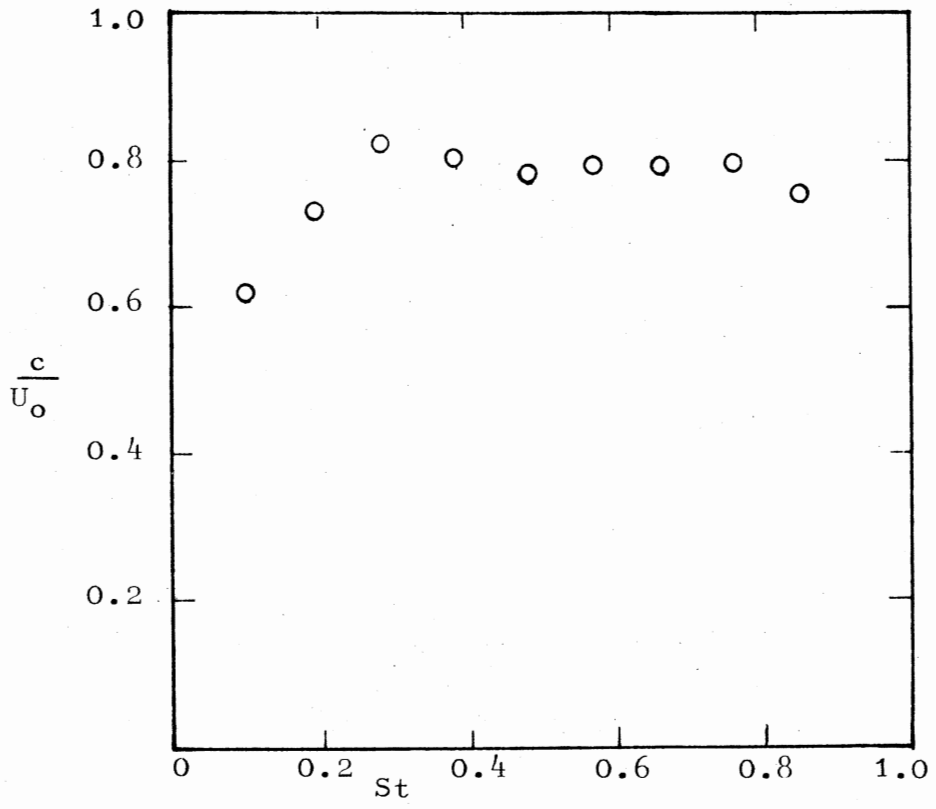

Figure 31. Axial Phase Velocities of Excited Disturbances

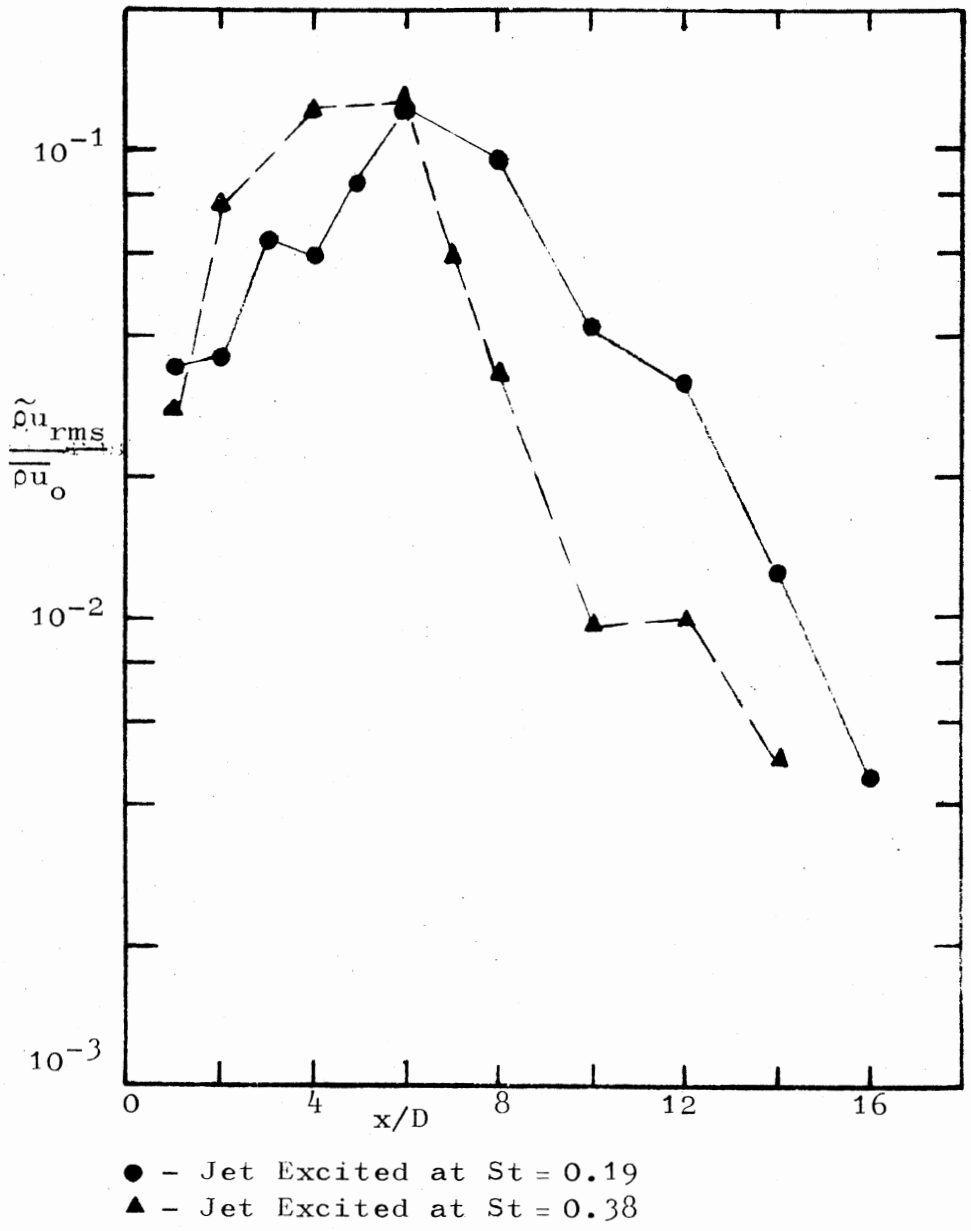

Figure 32. Coherent Mass-Velocity Fluctuation Amplitude in the Jet Shear Layer

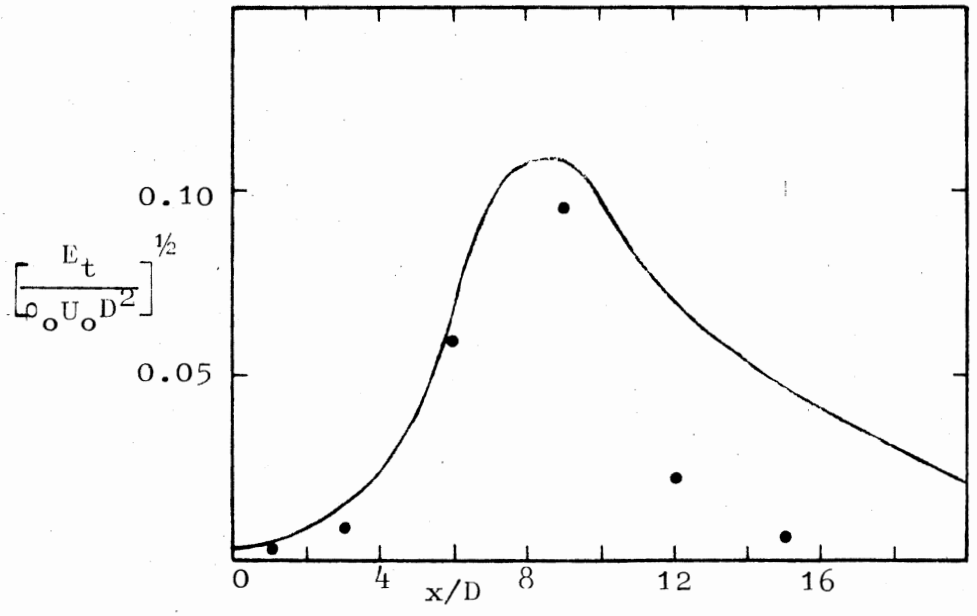

● - Present experiments

— - Tam (22) prediction

Figure 33. Integrated Coherent Energy Flux; Jet Excited at St = 0.19

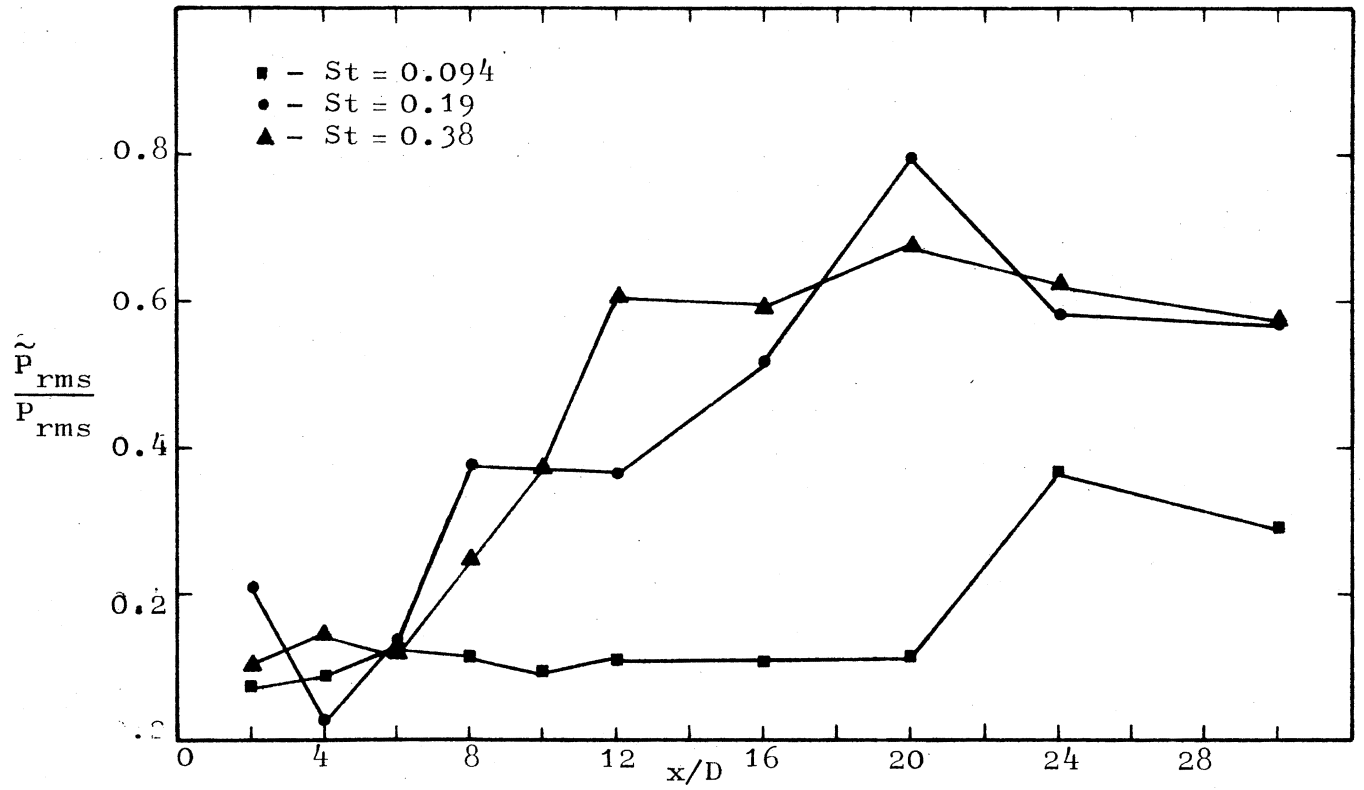

Figure 34. Coherent Sound Pressure Level; r/D = 8

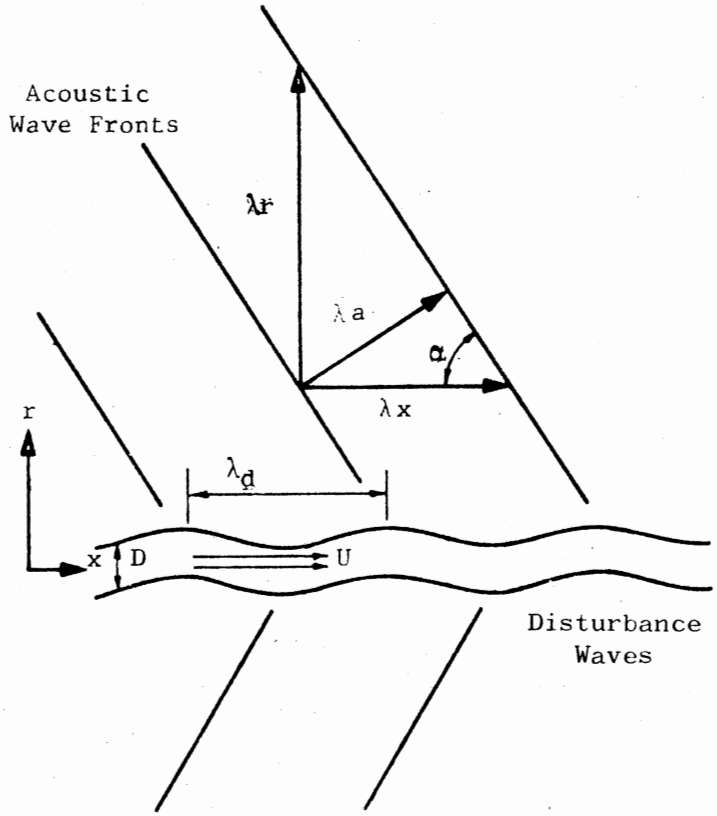

Figure 35. Orientation of Acoustic and Flow Disturbance Waves

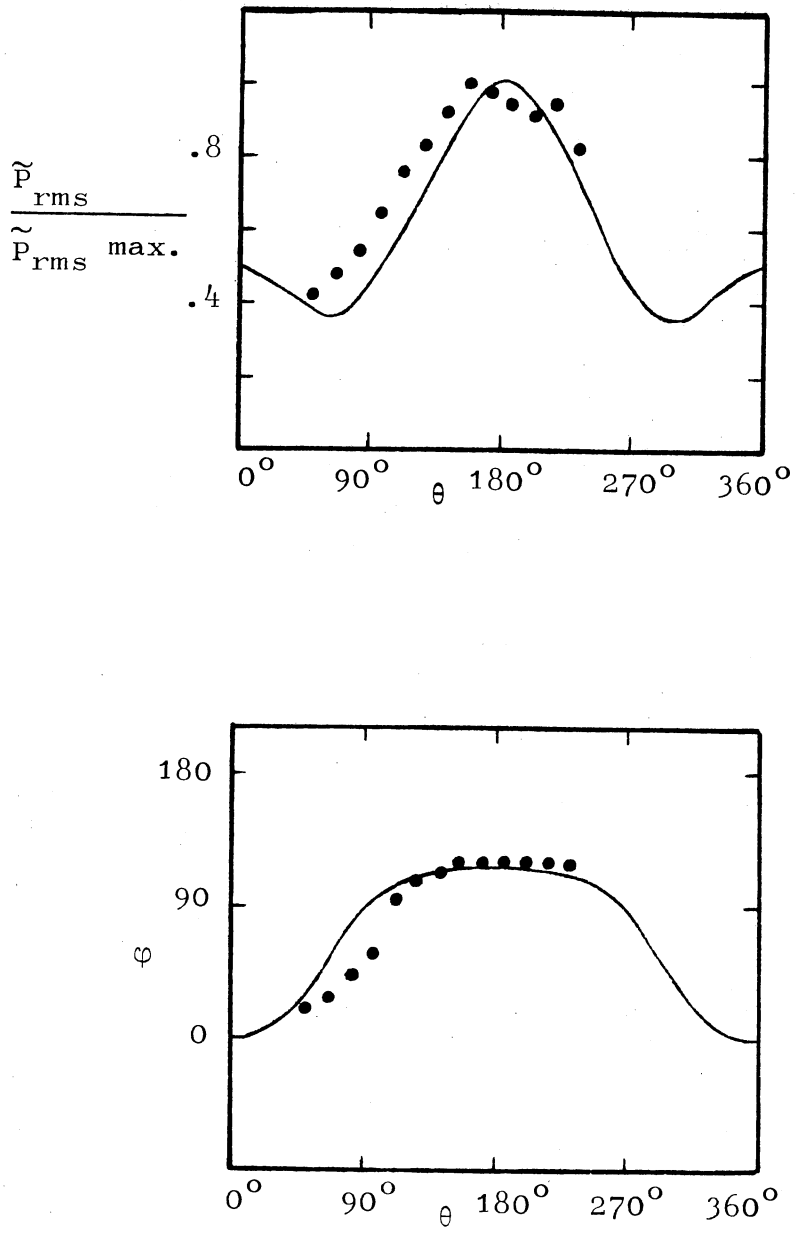

(a) Jet excited at St = 0.19

Figure 36. Coherent Sound Pressure Amplitude and Phase Angle as a Function of Azimuthal Angle

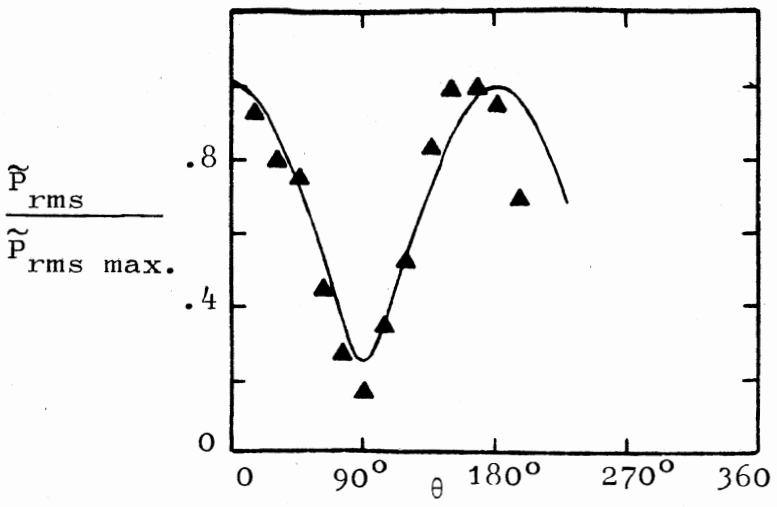

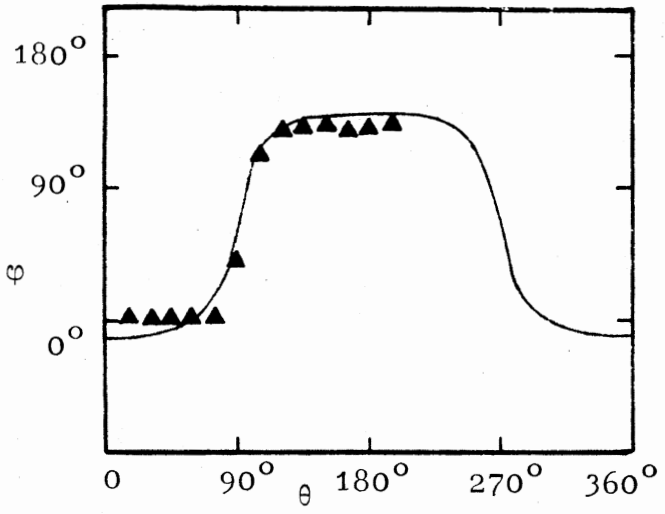

▲ - Experiment
(—) - Numerical Fit

(b) Jet excited at St = 0.38

Figure 36. (Continued)

APPENDIX B

TABLE

TABLE I

ACOUSTIC WAVELENGTH RESULTS

St	$\frac{\lambda_d}{D}$	$\frac{\lambda_x}{D}$	$\frac{\lambda_y}{D}$	μ degrees	α	C_a ft/sec	a_o ft/sec
0.19	3.85	4.35	4.87	63	48	1063	1128
0.38	2.11	2.10	3.15	54	56	1123	1128

VITA

Timothy Ray Troutt

Candidate for the Degree of

Doctor of Philosophy

Thesis: MEASUREMENTS ON THE FLOW AND ACOUSTIC PROPERTIES OF A MODERATE REYNOLDS NUMBER SUPERSONIC JET

Major Field: Mechanical Engineering

Biographical:

Personal Data: Born in Cherokee, Oklahoma, August 28, 1950, the son of Mr. and Mrs. Ray Troutt.

Education: Graduated from Helena High School in May, 1968; received Bachelor of Science degree in Physics from Oklahoma State University, Stillwater, Oklahoma, in May, 1972; received Master of Science degree from Oklahoma State University in May, 1974, and completed requirements for the Degree of Doctor of Philosophy, July, 1978.

Honors: Regent's Scholarship, Phi Kappa Phi Scholarship, Member of Phi Kappa Phi.

Professional Societies: American Institute of Aeronautics and Astronautics, Acoustical Society of America.